2017

Comprehensive Dual Liquid Chromatography with Quadruple Mass Spectrometry (LC1MS2 × LC1MS2 = LC2MS4) for Analysis of *Parinari Curatellifolia* and Other Seed Oil Triacylglycerols

William C. Byrdwell
USDA-ARS, c.byrdwell@ars.usda.gov

analytical chemistry

Article

pubs.acs.org/ac

Comprehensive Dual Liquid Chromatography with Quadruple Mass Spectrometry (LC1MS2 × LC1MS2 = LC2MS4) for Analysis of *Parinari Curatellifolia* and Other Seed Oil Triacylglycerols

William C. Byrdwell*

Food Composition and Methods Development Lab, Agricultural Research Service, Beltsville Human Nutrition Research Center, USDA, 10300 Baltimore Avenue, Building 161, Beltsville, Maryland 20705, United States

Supporting Information

ABSTRACT: Online two-dimensional (2D) comprehensive liquid chromatography (LC × LC) has become increasingly popular. Most LC × LC separations employ one or more detectors at the outlet of the second dimension, ^{2}D, with very short runs to avoid undersampling. We used six detectors, including dual parallel mass spectrometry (LC1MS2), for detection of the first dimension, ^{1}D. We made an argentation (silver-ion) UHPLC column from a strong cation exchange column for ^{2}D, coupled with UV and LC1MS2 detection. LC1MS2 in ^{1}D combined with LC1MS2 in ^{2}D, plus five other detectors, constituted LC2MS4 in a comprehensive LC1MS2 × LC1MS2 2D-LC separation. Electrospray ionization (ESI) high resolution accurate mass (HRAM) mass spectrometry (MS) and atmospheric pressure chemical ionization (APCI) MS were used in parallel for ^{1}D detection, while atmospheric pressure photoionization (APPI) MS and ESI-MS were used for detection of ^{2}D. The LC1MS2 used for ^{1}D allowed quantification of triacylglycerol (TAG) molecular species of *Parinari curatellifolia* and other seed oils, while the ^{2}D allowed isomers of TAG containing 18:3 fatty acyl chains as well as TAG regioisomers to be separated and identified. The LC1MS2 in ^{1}D allowed identification of oxo-TAG species by HRAM MS and quantification of 806.3 ± 1.3 and 1101 ± 22 μg/g of α- and γ-tocopherols, respectively, in *P. curatellifolia* by APCI-MS. It is now feasible to use silver-ion UHPLC as the ^{2}D separation in LC × LC and to use multiple mass spectrometers across both dimensions to perform conventional quantitative analysis and to take advantage of the newest LC × LC separation technology to identify isomers that are otherwise difficult to separate.

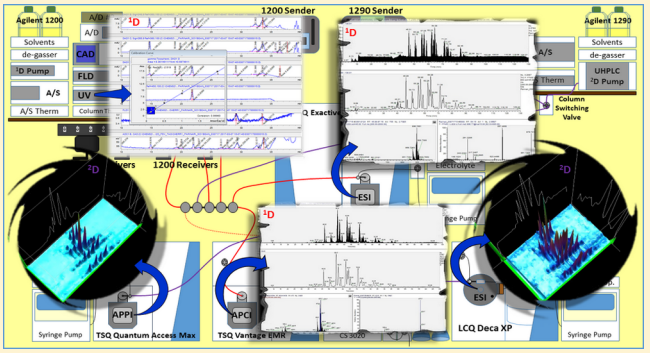

Numerous reviews of two-dimensional liquid chromatography (2D-LC) techniques have appeared in recent years, with those covering basic theory and principles[1−3] and describing 2D-LC coupled to mass spectrometry[4] (MS) being especially useful for the work described herein. Excellent chapters describing both theoretical and practical aspects with citations for numerous reviews and applications in a wide range of fields have recently appeared.[5,6] Note that the nomenclature of Marriott et al.[7] and Schoenmakers et al.,[8] as reflected in the chapter by Stoll,[6] is used here. Although the peak capacity in LC × LC is theoretically multiplicative (the product of the 1D-LC peak capacities) if the 2D separations are perfectly orthogonal, but in practice the maximum theoretical peak capacity is rarely achieved.[6] Nevertheless, it is typically possible to achieve a higher (often much higher) peak capacity by employing 2D-LC rather than 1D-LC.

Conventional LC × LC is typically done by using a low flow rate in the ^{1}D, which is all directed to the ^{2}D. The low flow rate helps minimize solvent incompatibility with the ^{2}D solvent system and provides wider peaks to allow more fractions to be taken across the ^{1}D peaks, which minimizes undersampling and limits the sample amount on the ^{2}D column to facilitate peak refocusing. 2D-LC often uses very high flow rates in the ^{2}D to provide very fast runs so that several 2D runs can be accomplished over the width of a 1D peak to adequately reconstruct the peak profile. As Davis, Stoll, and Carr[9] discussed elsewhere, undersampling results when too few samples are taken across a peak.

Mondello and co-workers[10−12] have pioneered the use of comprehensive LC × LC for triacylglycerols (TAG) using Ag-ion chromatography, which does a partial separation into groups by degree of unsaturation coupled to nonaqueous reversed-phase (NARP) HPLC, which further separates into distinct peaks by partition number (PN), where the PN = # carbons − 2 × # double bonds. Their work included the use of atmospheric pressure chemical ionization (APCI) MS for detection. Others soon followed with solvent modifications, etc., aimed at providing improved separations,[13] and a variety of lipid applications.[14−18]

Received: July 14, 2017
Accepted: August 29, 2017
Published: August 29, 2017

DOI: 10.1021/acs.analchem.7b02753
Anal. Chem. 2017, 89, 10537−10546

One thing that most methods for TAG analysis by 2D-LC have in common is the use of silver-ion chromatography in the ^{1}D, followed by NARP UHPLC in the ^{2}D. This is due in large part to the commercial availability of silver-ion HPLC columns and the lack of availability of silver-ion UHPLC columns (and even a dearth of strong cation exchange (SCX) UHPLC columns from which to make silver-ion columns). Unfortunately, Ag-ion HPLC produces clusters of peaks, with TAGs having similar degrees of unsaturation appearing in only partially resolved clusters. This puts a greater demand on the ^{2}D NARP-UHPLC separation to resolve those clusters.

In contrast, we already had a NARP-HPLC separation[19] that we liked for 1D-LC and just wanted to use Ag-ion UHPLC to tease apart a few remaining overlaps and separate isomers. Therefore, we made our own silver-ion UHPLC column from one of the few SCX columns available, which we loaded with silver using an approach that differs from the classic approach that is still commonly used.[20] Our standard NARP-HPLC method[19] utilized a substantial amount of ACN, which caused a lack of retention on the silver-ion UHPLC column. Thus, we implemented a methanol/ethanol/dichloromethane (MeOH/EtOH/DCM) gradient for NARP-HPLC that is compatible with the Ag-ion second dimension. The resolution is not quite as good as our standard MeOH/ACN/DCM method, but this is compensated for by the separation in the ^{2}D.

Due to our earlier interest in the α-eleostearic acid (α-EA) (9*Z*,11*E*,13*E*-octadecatrienoic acid)-containing TAGs in the seed oil of cherry (*Prunus cerasus*) pit oil (CPO), the new approach was applied to the same CPO and to parinari (African Mobola Plum, *Parinari curatellifolia*) seed oil (PSO) and wild soybean (*Glycine soja*) oil (SBO). Primary emphasis is on PSO because, in addition to general nutrition parameters[21,22] (protein, fiber, moisture, ash, total fat), little more than the fatty acid (FA) composition has been previously reported,[21] with that being erroneous or incomplete, although some limited data for related species are also reported. There has been reference to α-EA in other parinari species,[23−25] which contributed to our interest in the samples reported here. We also extend our previous approach[19] beyond vitamin D analysis to other fat-soluble vitamins, specifically tocopherols in all three seed oils.

We report here the first demonstration of comprehensive 2D-LC with double dual parallel mass spectrometry. Two mass spectrometers operated in APCI-MS and ESI-high resolution accurate mass (HRAM)-MS modes as well as UV, a fluorescence detector (FLD), corona charged aerosol detector (CAD), and an evaporative light scattering detector (ELSD) were used to monitor the first dimension, coupled with two other mass spectrometers operated in atmospheric pressure photoionization (APPI)-MS and ESI-MS modes plus UV, for a comprehensive LC2MS4 (or LC1MS2 × LC1MS2) analysis. This approach allowed the first report of the diacylglycerol (DAG) and TAG composition of PSO, identification of a previously unreported oxo-FA, and the first report and quantification of tocopherols in PSO and improved analysis of tocopherols in CPO. Results were supplemented and confirmed by gas chromatography (GC) with a flame ionization detector (FID) and GC-MS in electron impact (EI) and chemical ionization (CI) modes.

EXPERIMENTAL SECTION

Due to the number of instruments used for LC2MS4, most instrument details are provided in the Supporting Information.

Column Preparation. An Epic-SCX strong cation exchange (SCX) column, 100 × 2.1 mm, 3 μm particles (#122191-ESCX), was obtained from ES Industries, Inc. An old Constametric 4100 MS quaternary HPLC pump was used to flush the SCX column with Millipore D.I. H_2O for at least an hour at 0.2 mL/min. Then, a 500 mL bottle of 1.0 M $AgNO_3$ solution (Sigma-Aldrich) was fitted with a cap and line and fed directly into the Y-fitting supplying the reciprocating pump heads. Initially, the outlet of the column was sent to waste; then, after ∼30 min, the outlet was directed back into the $AgNO_3$ bottle. The system was located in a room with subdued light, and the bottle of $AgNO_3$ was placed inside two closed nested boxes to eliminate light exposure. The solution was allowed to recycle through the column overnight at 0.2 mL/min, which represented ∼450 column volumes over 13 h. Next, the $AgNO_3$ was removed, and the column was flushed with D.I. H_2O at 0.2 mL/min for at least an hour. Finally, the column was flushed with MeOH at 0.2 mL/min for an hour, after which it was ready for use.

2D-LC Instrumentation. An Agilent 1200 HPLC system that employed two Inertsil ODS-2 columns in series, 250 × 4.6 mm, 5 μm particles, which has been described previously,[19] was used for the ^{1}D separation. A fluorescence detector (FLD) was added between the diode array detector (DAD) and flow splitter since the earlier report. A splitting system controlled flow to each detector based on the length and I.D. of the fused silica capillary directed to each instrument. Full details of all components are provided in the Supporting Information and are depicted in Figure 1. In summary, the ^{1}D was monitored

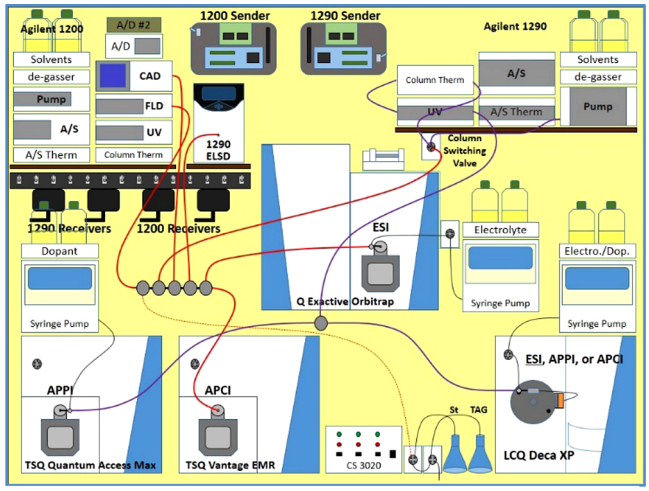

Figure 1. LC1MS4 configuration of instruments for comprehensive LC1MS2 × LC1MS2 plus UV, FLD, CAD, and ELSD.

using detection by a DAD, the FLD, the CAD, the ELSD (data not shown), a TSQ Vantage EMR mass spectrometer operated in APCI-MS mode, and a Q Exactive HRAM instrument operated in ESI-MS mode (with 20 mM NH_4OCOH in ACN, 1:4, at 20 μL/min via syringe pump). One branch of the splitter, having a flow rate of 53.67 μL/min, was directed to the Agilent G1170A switching valve with two 100 μL sample loops installed, producing a loop fill time of 1.86 min and modulation time of 1.91 min. The switching valve served as the interface to

DOI: 10.1021/acs.analchem.7b02753
Anal. Chem. 2017, 89, 10537−10546

an Agilent 1290 UHPLC system composed of a binary pump, column oven with the Epic-SCX/Ag-ion column installed, and DAD. Flow after the DAD no. 2 was directed to a single Valco tee splitter, with the two branches going to a TSQ Quantum Access Max mass spectrometer operated in APPI-MS mode with acetone dopant supplied by a dual piston syringe pump at 50 μL/min and an LCQ Deca XP ion trap mass spectrometer operated in ESI mode with 50 μL/min NH_4OCOH via syringe pump. Syringe pumps were AB140B/C dual piston syringe pumps. Syringe pumps for ESI instruments were plumbed through electronically controlled valves attached or built into the instruments to flush deionized water (from old HPLC pumps) through the sources between runs to reduce problems with clogging. Control of all instruments was coordinated using the 14-switch wireless communication contact closure system (WCCCS) previously described.[26] Visualization of the 2D-LC chromatograms was done using LC Image v. 2.5b7 software from GC Image, Inc.

GC Instrumentation. Analyses on an Agilent 6890N GC with a FID and an Agilent 7890A GC with 5975C MS (in EI and CI modes) were performed using the instruments and conditions recently reported.[27] Column and flow conditions are given in the Supporting Information.

Quantification. Calibration levels of 0.125, 0.250, 0.500, 1.00, and 2.00 μg/mL were prepared from 25.0 μg/mL (nominal) stock solutions of each fat-soluble vitamin (FSV) listed below with each concentration adjusted for standard purity (from Certificates of Analysis) and precise stock solution concentration. d_6-α-Tocopherol at 1.00 μg/mL was added as IS to all standards and samples. Quantification of FSVs by MS was done using APCI-MS in time-segmented selected ion monitoring (SIM) and selected reaction monitoring (SRM) modes using the parameters listed in the Supporting Information. Quantification of DAGs and TAGs was done using the GC-FID response-factor-adjusted approach previously described,[28,29] with inclusion of 1×^{13}C isotopic peaks for added sensitivity without loss of specificity, as previously discussed.[30] Quantification of FSVs by UV detection was done using wavelengths adapted from Ball,[31] specifically 297 nm for α-, γ-, and δ-tocopherols, 265 nm for vitamin D_2 and D_3, 326 nm for retinol (vitamin A), retinyl acetate, and retinyl palmitate, and 248 nm for phylloquinone (vitamin K_1). Fluorescence detection of tocopherols was done using a legacy detector (Agilent 1100 series) at 330 nm as a test of FLD specificity. Additional parameters for UV and FLD are given in the Supporting Information. All peaks were manually integrated, and calculations were performed using the linest() function in Excel spreadsheets using both IS and external standard approaches (ES).[19,30] Because the IS was optimized for MS detection, results by UV could only be estimated as discussed below.

RESULTS

We bypassed the problem of under-sampling and problems associated with quantification of 2D-LC "blobs" by directly monitoring the ^{1}D using two mass spectrometers, operated in APCI-MS and ESI-HRAM-MS modes as well as UV, FLD, CAD, and ELSD. Chromatograms and calibration lines of α-tocopherol by ^{1}D SIM and SRM are shown in Figure 2. Although we did not know to expect tocopherols in PSO, we routinely run samples using our FSV and TAG screening procedure, which allows quantification of any of the FSVs mentioned above if they are present. Table 1 shows the results

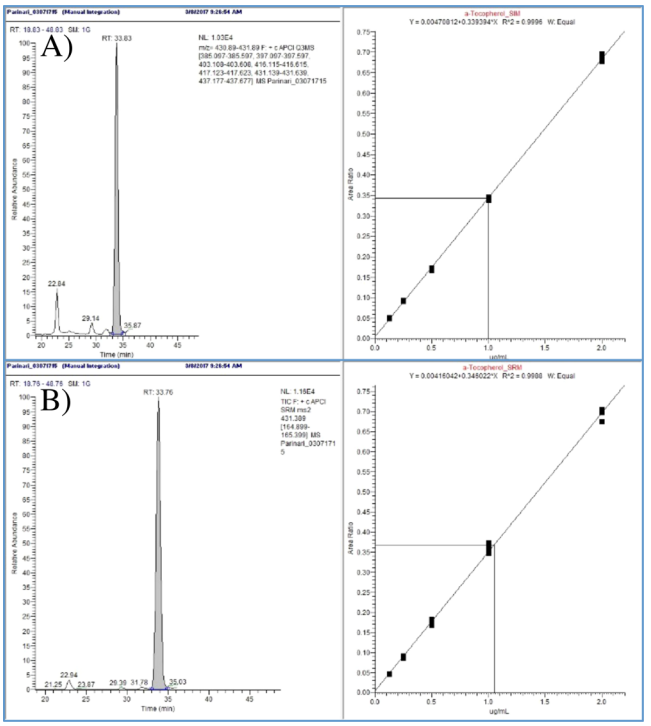

Figure 2. Chromatograms and calibration lines for α-tocopherol by (A) selected ion monitoring and (B) selected reaction monitoring. FA abbreviations: P, palmitic acid, 16:0 (carbons:double bonds); El, α-eleostearic acid, 9*c*,11*t*,13*t*-18:3 (*c* = cis, *t* = trans); L, linoleic acid, 18:2; O, oleic acid, 18:1; S, stearic acid, 18:0; G, gadoleic acid, 20:1; A, arachidic acid, 20:0.

Table 1. Quantification of α-, γ-, and δ-Tocopherols by SIM and SRM APCI-MS in ppm (μg/g Oil)

Selected ion monitoring, internal standard method						
	α	SD	γ	SD	δ	SD
cherry	293.5	3.5	630	26	97	14
parinari	789	28	881	45	6	16
soybean	29.9	0.3	168	14	227	13
r^2	0.9996		0.9883		0.9917	
Selected reaction monitoring, internal standard method						
	α	SD	γ	SD	δ	SD
cherry	281	12	897.8	5.4	120.8	6.9
parinari	806.3	1.3	1101	22	34.0	6.3
soybean	18.9	0.2	193.0	1.4	198	13
r^2	0.9988		0.9943		0.9956	

for the IS approach by SIM and SRM APCI-MS in ppm or μg/g of oil = mg/kg of oil with the first nonsignificant figure shown or to 0.1. The coefficients of determination (r^2) given in Table 1 indicate good linearity of the calibration lines. Results by the ES approach by APCI-MS and the IS and ES approaches by UV detection are given in the Supporting Information because these are all less desirable and reliable than the IS approach by MS. All ES and IS results by MS and UV, with the exception of UV results for α-tocopherol in PSO, were in good to excellent agreement among all approaches. To derive an estimation of IS results by UV required approximation of the IS integrated areas for 1.00 μg/mL as follows: the area for each α-tocopherol calibration standard was divided by the α-tocopherol total amount to give (area/(μg/mL)). Each area for all other FSVs was divided by the same-run normalized IS area. For samples,

DOI: 10.1021/acs.analchem.7b02753
Anal. Chem. 2017, 89, 10537−10546

the average normalized signal area across all standards (= 5.5294 ± 0.6330) was used as the IS area because it was unknown how much of the α-tocopherol was attributable to the IS and how much came from the oil sample. Again, no such approximation was required for results by ES or IS by MS or ES by UV.

FAs, DAGs, and TAGs. The FA composition calculated from the sum of response-factor-normalized DAGs and TAGs and by GC-FID for FAs present at ≥0.1% for *P. curatellifolia* is given in Table 2. Due to space limitations, all 18:3 species are grouped together in Table 2, as are all oxo-18:3 FA. A more detailed composition is provided in the Supporting Information. As identified by GC-MS and quantified by GC-FID, 90.0 ± 0.1% of 18:3 was α-eleostearic acid, 7.6 ± 0.1% was β-El, a third isomer (unidentified) represented 1.7 ± 0.0%, and only 0.1 ± 0.0% was normal Ln, and these comprise almost all of the 48.8% in Table 2. While eleostearic acid has been reported previously, this represents the first report of oxo-eleostearic acid in *P. curatellifolia*. Four oxo-El isomers were found by GC-MS and quantified by GC-FID, with the two major isomers representing 81.0 ± 0.8% and 13.3 ± 0.3%, comprising the majority of the 1.5% of oxo-El shown in Table 2. The compositions of DAGs and TAGs are given for the first time in Tables 3 and 4, respectively. DAGs represented only 1.52% of the total area of DAGs and TAGs. Figure 3 shows an ESI-HRAM-MS chromatogram and mass spectra of eleostearic acid and two oxygen functional group containing TAGs, and Figure 4 shows the APCI-MS data acquired in parallel. The $[M+NH_4]^+$ and $[M+H]^+$ ions for several TAGs had unexpected masses that were 14 mass units higher than those of normal eleostearic acid containing TAGs, with accompanying $[DAG]^+$ fragments at *m/z* 609.450 ($[ElEl+14]^+$). This mass difference could represent either a branched methyl-containing FA (−H + CH_3 = 14.0157) or an oxo-FA (−2H + O = 13.9793). Direct detection by HRAM ESI-MS in the ^{1}D allowed unambiguous differentiation of these two possibilities. The mass accuracy for normal, known TAGs were in the 2−4 ppm range, while for the possible methylated TAGs, the mass differences were 42−45 ppm for the $[M+NH_4]^+$ peaks and 62−63 ppm for the *m/z* 609.450 $[DAG]^+$ fragment. On the other hand, the calculated accurate masses for the oxo-eleostearic TAGs were within the 2−4 ppm range for all $[M+NH_4]^+$ and $[DAG]^+$ fragments (normal and ox-El), providing very strong evidence that the unknown TAG molecular species contained oxo-eleostearic acid. GC-MS chromatograms (not shown) exhibited a corresponding peak at *m/z* 306.2 representing the oxo-18:3 FAME. Finally, the chromatographic behavior of oxo-TAGs, which eluted prior to normal TAGs on the RP-HPLC column due to increased polarity, is consistent with expected behavior under RP-HPLC conditions. Several steps were taken to confirm that the oxo-TAGs were endogenous native species and were not formed during extraction. All data confirm the identification of multiple DAG and TAG molecular species containing oxo-eleostearic acid, shown in Tables 3 and 4, with oxo-TAGs being 4.65% of the response-factor-normalized TAG integrated area. The exact type and location of the oxo-

Table 2. FA Composition Calculated from DAG and TAG Composition of *P. cuatellifolia* Compared to FA from GC-FID of FA Methyl Esters

FA	average (%)	SD (%)	GC-FID (%)
P	9.1	0.0	9.3
El	48.8	0.1	48.8
L	14.4	0.1	14.0
O	17.7	0.1	17.5
S	7.3	0.1	7.6
A	0.4	0.0	0.4
G	0.7	0.0	0.7
oxo-El	1.6	0.0	1.5
sum	99.9		99.9

Table 3. Response Factor Normalized DAG Composition for *P. curatellifolia*

DAG	RT (1)[a]	% comp	DAG pk. 2/1[b]
oxElEl	19.09	0.7	0.21
oxElL	21.09	0.1	0.28
oxElO	26.30	0.2	0.23
oxElP	26.59	0.1	0.30
ElEl	32.46	17.4	2.57
PoO	35.68	0.8	1.61
LEl	35.84	11.2	2.72
LL	37.60	11.7	4.19
OEl	39.02	12.5	1.57
OL	39.77	14.7	3.43
PL	39.96	6.8	1.53
OO	41.73	6.9	1.50
OP	42.00	7.0	0.72
SL	42.55	4.8	1.59
OS	44.99	5.1	0.52
sum	99.9%		

[a]Retention time for first peak of the pair. [b]Ratio of DAG peak 2 to DAG peak 1.

Table 4. Response Factor Normalized TAG Composition for *P. curatellifolia*

TAG	RT	% comp	TAG	RT	% comp
oxElElEl	46.02	1.3	POL	75.30	2.1
oxElElL	47.08	0.4	LLS	76.15	0.5
oxElElO	50.54	0.9	PPL	77.15	0.7
oxElElP	51.23	0.7	LElA	79.48	0.3
oxElLO	51.87	0.1	ElElA	79.89	0.5
oxElOO	56.21	0.1	SOEl	82.19	3.0
oxElElS	56.26	0.9	OOO	82.21	1.0
oxElOP	56.83	0.1	OLG	82.29	0.3
oxElOS	63.36	0.1	OOP	84.24	1.4
ElElEl	55.11	12.0	ElSP	84.32	1.0
ElElL	56.70	8.3	PLG	84.37	0.2
LLEl	58.47	3.3	SLO	85.04	1.4
LLL	60.31	0.4	POP	86.29	0.5
ElElO	62.05	11.3	SLP	87.09	0.9
ElElP	63.23	8.1	OOG	90.98	0.1
OLEl	64.10	7.8	ElOA	91.46	0.1
PLEl	65.44	4.6	OOS	93.68	0.8
LLO	66.33	1.0	ElSS	93.83	0.9
LLP	67.64	0.9	POS	95.79	0.7
ElElG	68.65	1.3	PLA	96.36	0.1
ElElS	70.83	8.9	SSL	96.38	0.4
OOEl	70.94	4.2	PPS	99.31	0.1
POEl	72.50	3.0	POA	104.09	0.1
LLG	73.27	0.2	SSO	104.19	0.3
OOL	73.53	1.8	sum		99.3
PPEl	74.35	0.4	oxo-TAG		4.65

DOI: 10.1021/acs.analchem.7b02753
Anal. Chem. 2017, 89, 10537−10546

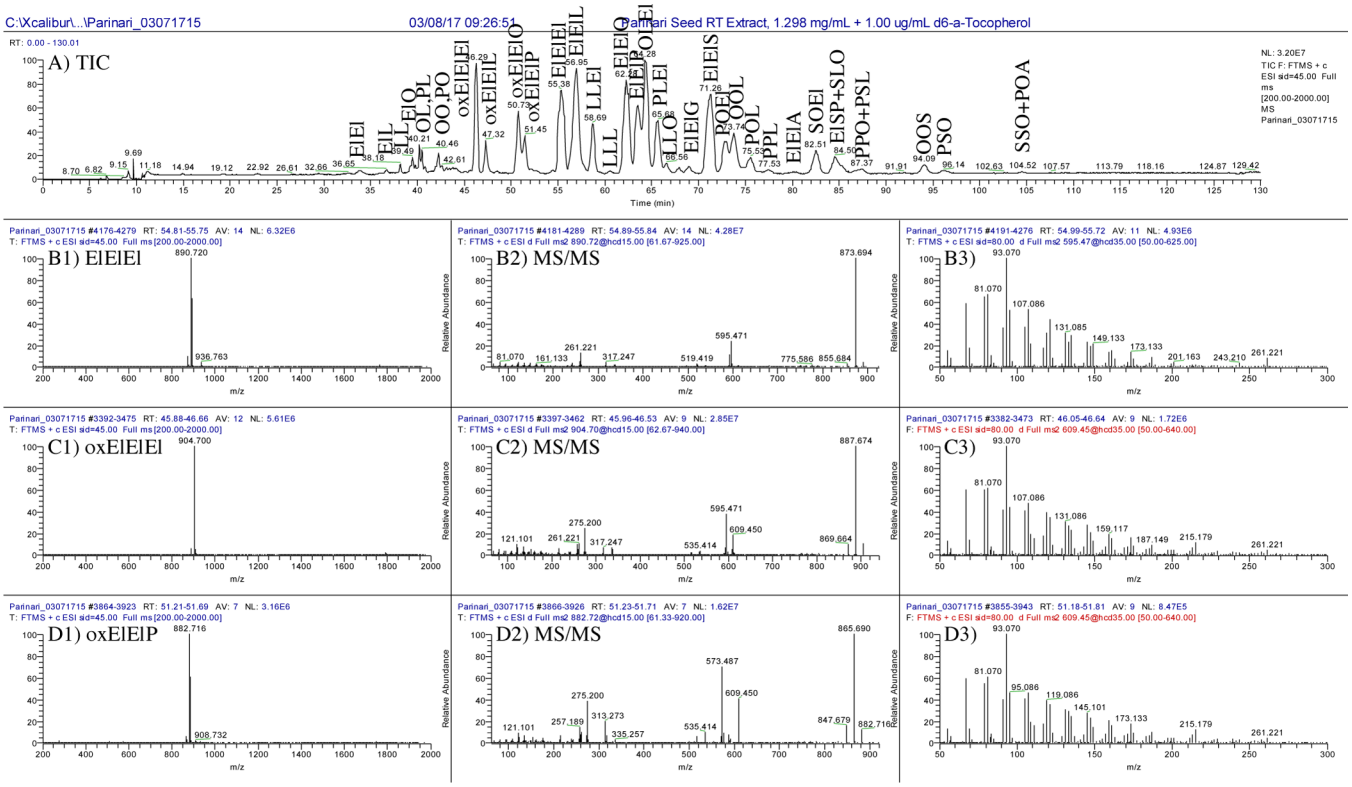

Figure 3. Q Exactive Orbitrap ESI-HRAM-MS total ion current chromatogram (TIC) and mass spectra for trieleostearin, ElElEl, and two TAGs containing previously unidentified oxo-eleostearic acid, oxElElEl, and oxElElP (column 1); low-energy CID MS/MS of $[M+NH_4]^+$ (column 2); and higher-energy CID of m/z 595 or m/z 609 $[DAG]^+$ fragment (column 3). FA abbreviations are in the Experimental Section.

functional group could not be determined from the mass spectra alone. However, comparison of the MS/MS spectra from ElElEl and oxElElEl in Figure 3 hint that the oxo-group is not at the distal end of the FA chain, and differences in the m/z 105−111 (= C_8H_x) and m/z 117−119 (= C_9H_x) peaks indicate the possibility that it is an 8,9-oxo group. Unfortunately, time, resources, and stakeholder interest will not allow us to pursue identification of the exact identity of this oxo-FA. The early eluting peaks should be collected and subjected to IR and NMR analysis. We will be happy to share all LC-MS data. Finally, there was both HRAM ESI-MS ($[M+NH_4]^+$= m/z 918.681 observed) and APCI-MS ($[M + H]^+$= m/z 901.6 obs) evidence for the dioxo TAG oxEloxElEl present at a very low level at earlier retention time, which was not quantified.

The FA, DAG, and TAG compositions for cherry pit and wild SBO are given in the Supporting Information because these have been reported previously and were used for verification of the new approach. All results for CPO are in good agreement with the results reported recently using 1D NARP-HPLC.[27] The SBO FA, DAG, and TAG compositions are similar to results reported elsewhere, although previous reports focused primarily on *Glycine max* commercially produced soybeans rather than the wild type.

Second-Dimension (^{2}D) Data. A contour plot for *P. curatellifolia* by silver-ion UHPLC with APPI-MS detection is shown in Figure 5 and that by ESI-MS is shown in Figure 6. Corresponding 3D plots are given in Figures 7 and 8. As usual, ESI-MS exhibits sensitivity greater than that of either APCI-MS or APPI-MS, giving larger peaks in Figures 6 and 8. No attempt was made to quantify the DAGs and TAGs using the contour plots because these are known to be problematic for quantification,[6,32−35] and very effective quantification using a well-established approach was provided by the ^{1}D APCI-MS data. The ^{2}D data were used only for qualitative analysis. The silver-ion UHPLC column provided a separation based on the well-known principles that have been described for argentation chromatography in the past. Boryana Nikolova-Damyanova and William W. Christie provide an excellent tutorial for argentation chromatography at the Lipid Library (http://lipidlibrary.aocs.org/content.cfm?ItemNumber=40341). Because *cis* double bonds produce stronger complexes with silver ions than *trans* double bonds,[36] the UHPLC column described here very effectively separated ElElEl containing all α-eleostearic acid from ElElEl containing a β-eleostearic acid FA, as seen in Figures 5 and 6. Thus, comprehensive NARP-HPLC × Ag-ion-UHPLC appears to be well-suited for differentiating *cis*/*trans* isomers in TAGs.

Also, the position of the unsaturated FAs in TAGs has a primary influence on the retention on the Ag-ion UHPLC column, with those in the outer positions, i.e. 1 and 3, having a stronger effect on retention than those in the middle, *sn*-2, position. For example, Figure 9 shows a ^{2}D UHPLC ESI-MS EIC for m/z 904.8, which represents multiple isobaric TAG molecular species and their isomers.

First, this shows that most peaks eluted in single, unsplit peaks, although some (e.g., OSO) straddled two modulation periods separated by the modulation time, as shown for OSO in Figure 9. This greatly simplified interpretation of data and gave the sharp peaks exemplified in Figures 7 and 8. Second, the silver-ion column readily differentiated between two oleic acid chains in the 1,2 positions in OOS from two oleic chains in the 1,3 positions in OSO. However, because retention was based on degree of unsaturation, with minimal effect of chain length, OSO and GPO, which both have two monounsaturated FAs in

DOI: 10.1021/acs.analchem.7b02753
Anal. Chem. 2017, 89, 10537−10546

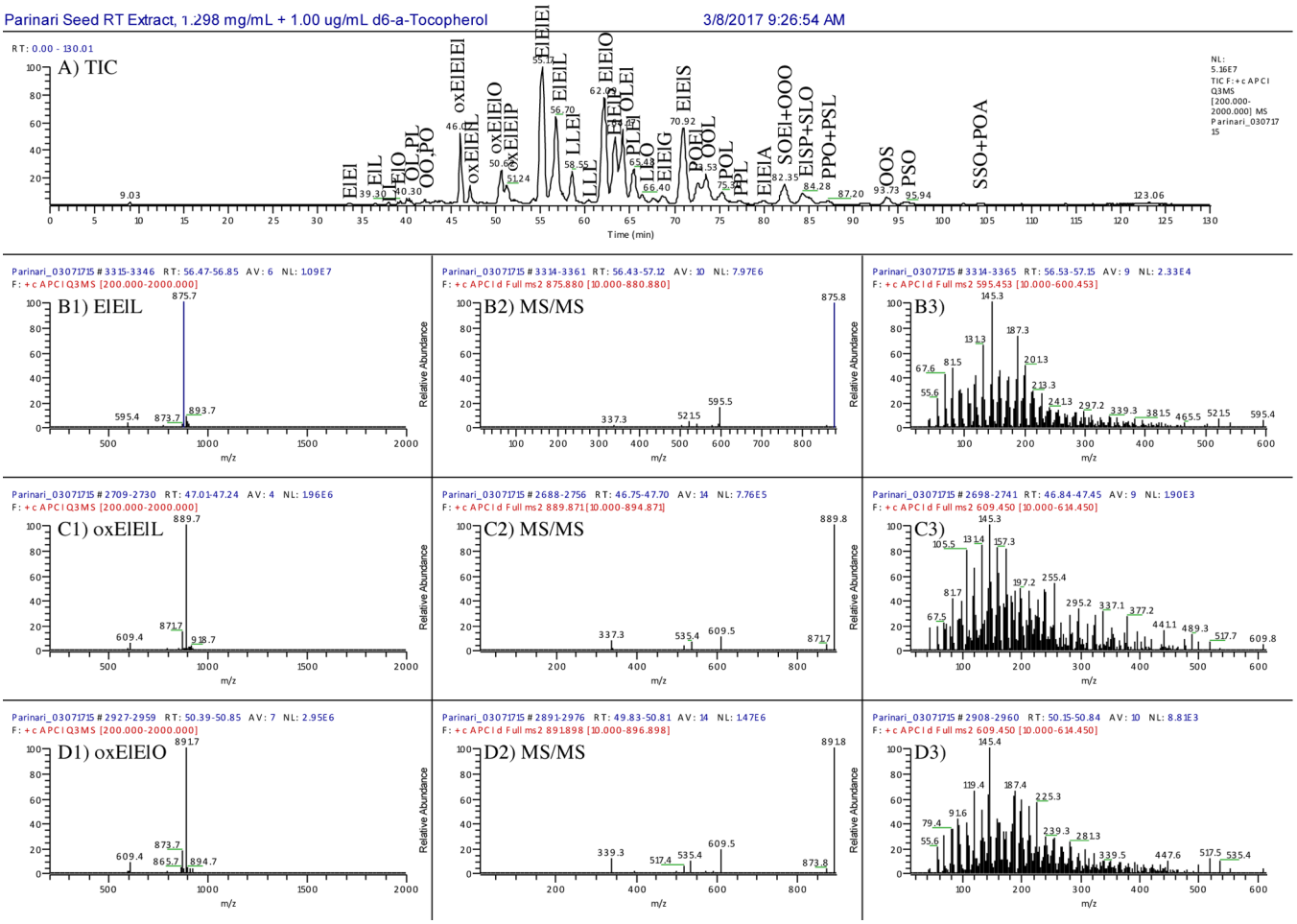

Figure 4. TSQ Vantage EMR APCI-MS TIC and mass spectra for ElElL, oxElElL, and oxElElO (column 1), low-energy CID MS/MS of $[M + H]^+$ (column 2), and higher-energy CID of m/z 595 or m/z 609 $[DAG]^+$ fragment (column 3). FA abbreviations are in the Experimental Section. See Table 4 for TAG composition from APCI-MS.

the 1,3 positions were not separated, although these could be distinguished by the different $[DAG]^+$ fragments despite having one $[DAG]^+$ fragment, m/z 605.5, and the protonated molecule mass in common. Similarly, SLS was differentiated from SSL due to the different position of the "L" FA. But SLS was not separated from PLA, which has different saturated FA chain lengths at 1 and 3, but the "L" FA in the same *sn*-2 position. In general, the first row of TAGs eluted in Figures 5 and 6 had one or no *cis* double bonds in one of the 1 or 3 positions with one or no *cis* double bonds in the *sn*-2 position, with the exception of oxo-El, in which the oxo- group appeared to reduce coordination of El with the Ag^+ and reduce retention (i.e., oxElElEl). The second row of TAGs had either two *cis* double bonds in the 1 or 3 positions or one diunsaturated FA (i.e., "L") in the *sn*-2 position. Additional unsaturation in the 1,3 positions had a greater influence on retention with additional unsaturation in the *sn*-2 position having a slightly lesser effect on retention, as mentioned above. Because APPI-MS and ESI-MS were used for detection in the ^{2}D, assignment of regioisomer identities by the Critical Ratio[37,38] $[AA]^+/[AB]^+$ by MS was less reliable[38] than by APCI-MS. For instance, the difference in $[OO]^+/[OS]^+$ between OOS sand OSO(2) in Figure 9 is not as large as expected or reported using APCI-MS.[39] Fortunately, Ag-ion UHPLC was very effective for separating regioisomers, reducing the need to rely on fragment ratios in ESI-MS/MS or APPI-MS mass spectra.

DISCUSSION

Although complete details are not given, Powell[40] described producing a silver-ion column from a sulfonate derivatized silica column by flowing silver nitrate through the column. Although we were not initially aware of that work, we used a similar approach, differing primarily in the fact that we employed exhaustive saturation by recycling $AgNO_3$ through a commercially available SCX column overnight. Both approaches contrast the more commonly used approach by Christie[20] of manually injecting $AgNO_3$ solution, which has been widely used to good effect. In the first sequence of runs immediately after preparation of a new column, small amounts of silver adducts were formed during ESI-MS, but these quickly disappeared with further use. No corrosive effects of $AgNO_3$ elution were observed in the ionization source of any instrument. This approach has been used both for 1.8 μm particle and 3.0 μm particle columns, but we prefer the latter for increased robustness.

It is important to emphasize that the excellent quantitative results reported here would not be possible using conventional comprehensive 2D-LC approaches. Quantification of ^{2}D 2D-LC data is an ongoing area of development,[32] but is not yet as straightforward as conventional integration of 1D or ^{1}D chromatograms. As mentioned by Place et al.,[33] each 2D peak consists of individual 1D chromatograms (slices) that

DOI: 10.1021/acs.analchem.7b02753
Anal. Chem. 2017, 89, 10537−10546

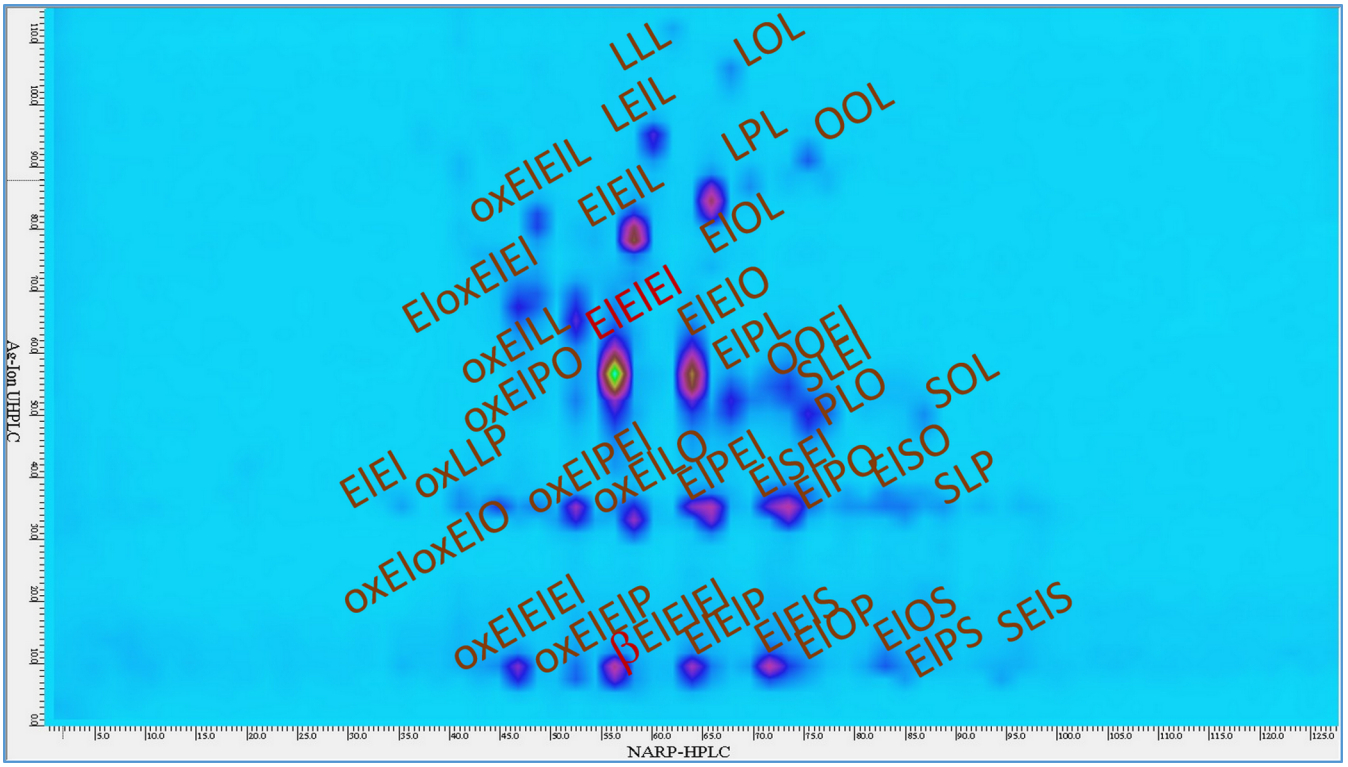

Figure 5. Second dimension silver-ion UHPLC separation with APPI-MS of *P. curatellifolia* seed oil.

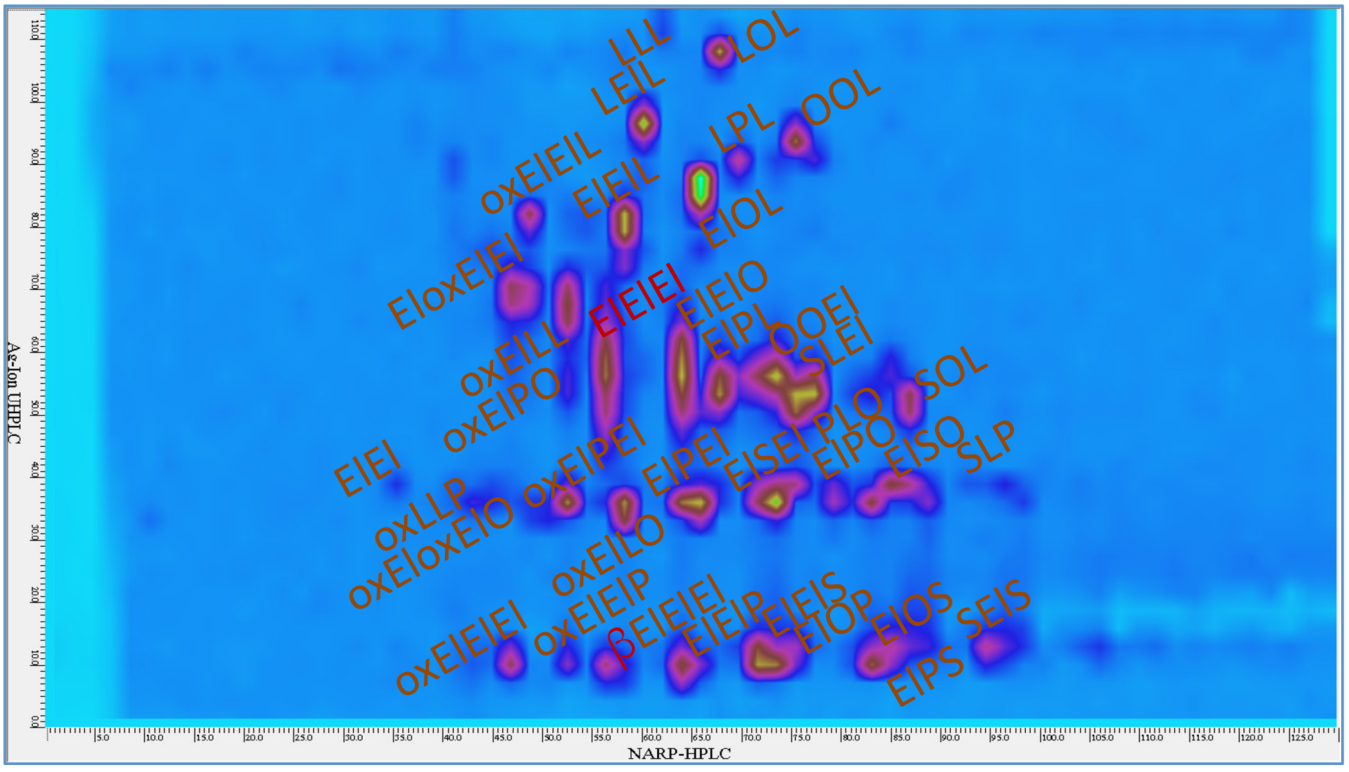

Figure 6. Second dimension silver-ion UHPLC separation with ESI-MS of *P. curatellifolia* seed oil.

would normally be manually integrated in 1D analysis. But having numerous slices across each 2D peak makes such integration impractical. So, they described several approaches for automated integration of 2D peaks, which involved lab-written procedures in the R programming language. Cook et al.[34] discussed the several-fold higher %RSDs encountered in 2D-LC and the reasons for these and many other factors, including the poorer S/N due to peak dilution caused by peak fractionation. They employed a single UV detector at the outlet of the ^{1}D, for 2D assisted LC, or 2DALC. Recently, targeted

DOI: 10.1021/acs.analchem.7b02753
Anal. Chem. 2017, 89, 10537−10546

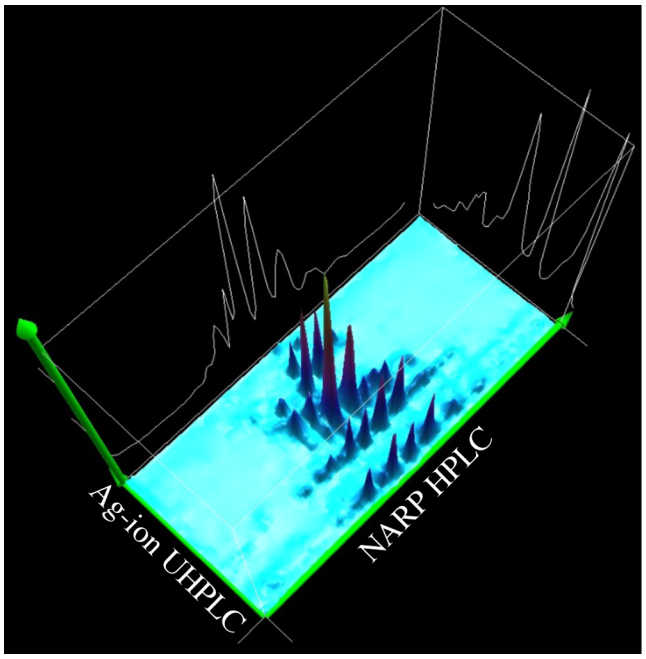

Figure 7. 3D plot of Ag-ion UHPLC APPI-MS for *P. curatellifolia*.

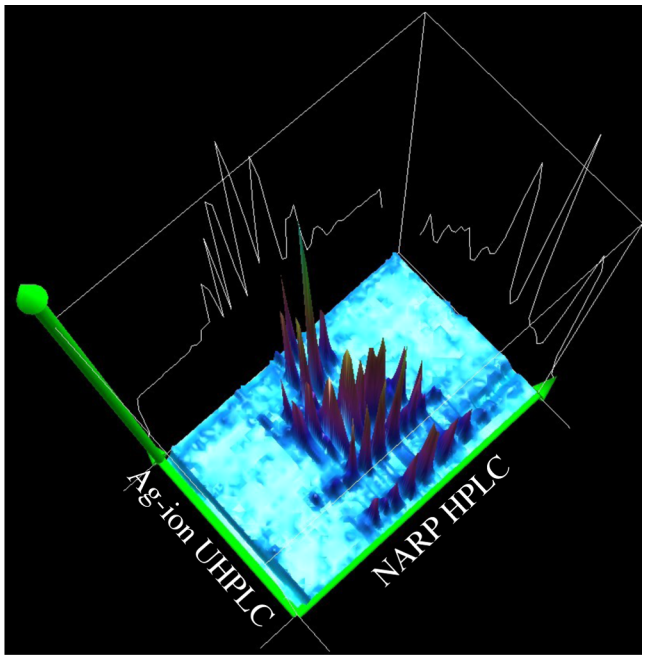

Figure 8. 3D plot of Ag-ion UHPLC ESI-MS for *P. curatellifolia*.

quantitative MS analysis of two target compounds using multiple reaction monitoring (MRM) was combined with qualitative analysis of wine polyphenols.[35] But because we wanted to quantify multiple FSVs and semiquantify a large number of DAGs and TAGs (by relative percentage composition), we took an approach similar to 2DALC but with many more detectors.

Quantification of CPO tocopherols was included because the extract-and-shoot approach gave values that were substantially higher than those values reported by a commercial lab in our recent report. The results reported earlier were obtained using the traditional approach to sterol analysis, involving heated saponification, extraction, and collection of unsaponifiable material and derivatization followed by GC-FID analysis. By eliminating all harsh and inefficient treatment such as saponification and derivatization, we observed higher levels. Additional work is underway to confirm these results by analysis of standard reference material 3278 from the National Institute of Standards and Technology. Furthermore, the use of both SIM and SRM (often thought of as the "gold standard" for analysis) MS provided very strong confirmation of tocopherol identity as well as quantity. Additionally, by obtaining survey MS and data-dependent MS/MS scans on all instruments, we are able to refute the presence of β-sitosterol that was reported by the same commercial lab using the same saponification, extraction and collection, and derivatization approach in CPO. Using APCI-MS EICs for a 5 Da mass range including γ-tocopherol (Table 1) ($[M + H]^+ = m/z$ 417.4) and β-sitosterol ($[M + H]^+ = m/z$ 415.4), we were able to clearly see the peaks for γ-tocopherol but not β-sitosterol. This demonstrates that peaks at a given retention time by GC without confirmation by MS, especially after extensive chemical pretreatment, are not sufficient for identification and quantification. Thus, it is advisible to view commercial lab results that do not include MS with healthy skepticism. Similar skepticism should be applied to SIM versus SRM results. Any interfering species that produce fragments or other ions similar to target compounds can skew SIM results. SRM is a more selective process, providing a higher degree of confidence. Nevertheless, because this approach has not yet been validated using a standard reference material (underway), these results for tocopherols are preliminary results.

Skepticism was also applied to observation of the oxo-FA, oxo-DAGs, and oxo-TAGs. To prove that these were not produced by oxidation during the Folch extraction process, we conducted experiments in which all solvents were deaerated with argon, and extractions were done using both cold solvents and room temperature solvents. The oxo-DAGs and oxo-TAGs were present in all samples regardless of treatment. Thus, we can conclude that these did contain uncommon oxo-FAs. We doubt that these are hydroxyl-FAs because they lack the very common dehydration products, $-H_2O = \Delta 18$ Da, that appear with large abundances in ESI-MS/MS and APCI-MS spectra of hydroxyl-TAGs.[41,42]

It should be pointed out that the ^{2}D solvent system (MeOH/ACN) is entirely compatible and miscible with the ^{1}D solvent system (MeOH/EtOH/DCM), thereby eliminating all compatibility issues that can arise using hexane-based solvent systems for Ag-ion HPLC. Also, the column-switching valve was plumbed in countercurrent mode (first in, last out) because the polyunsaturated TAGs that eluted first in the ^{1}D eluted last in the ^{2}D. Furthermore, *cis*-polyunsaturated DAGs and TAGs did not elute from the Ag-ion UHPLC column until the ACN content reached a sufficient level, so there was a degree of sample reconcentration at the head of the column, contributing to the sharp peaks seen in Figures 7 and 8.

When referring to the 1 and 3 positions of the glycerol backbone, we no longer use the designation *sn* (stereospecific numbering), because NARP HPLC, Ag-ion UHPLC, ESI-MS, APCI-MS, and APPI-MS are not capable of distinguishing enantiomers. The only position that can be known from these data is the *sn*-2 position. Chiral chromatography is required to differentiate the *sn*-1 and *sn*-3 positions. Therefore, the labels for the 1 and 3 positions are interchangeable unless chiral chromatography has been applied.

DOI: 10.1021/acs.analchem.7b02753
Anal. Chem. 2017, 89, 10537−10546

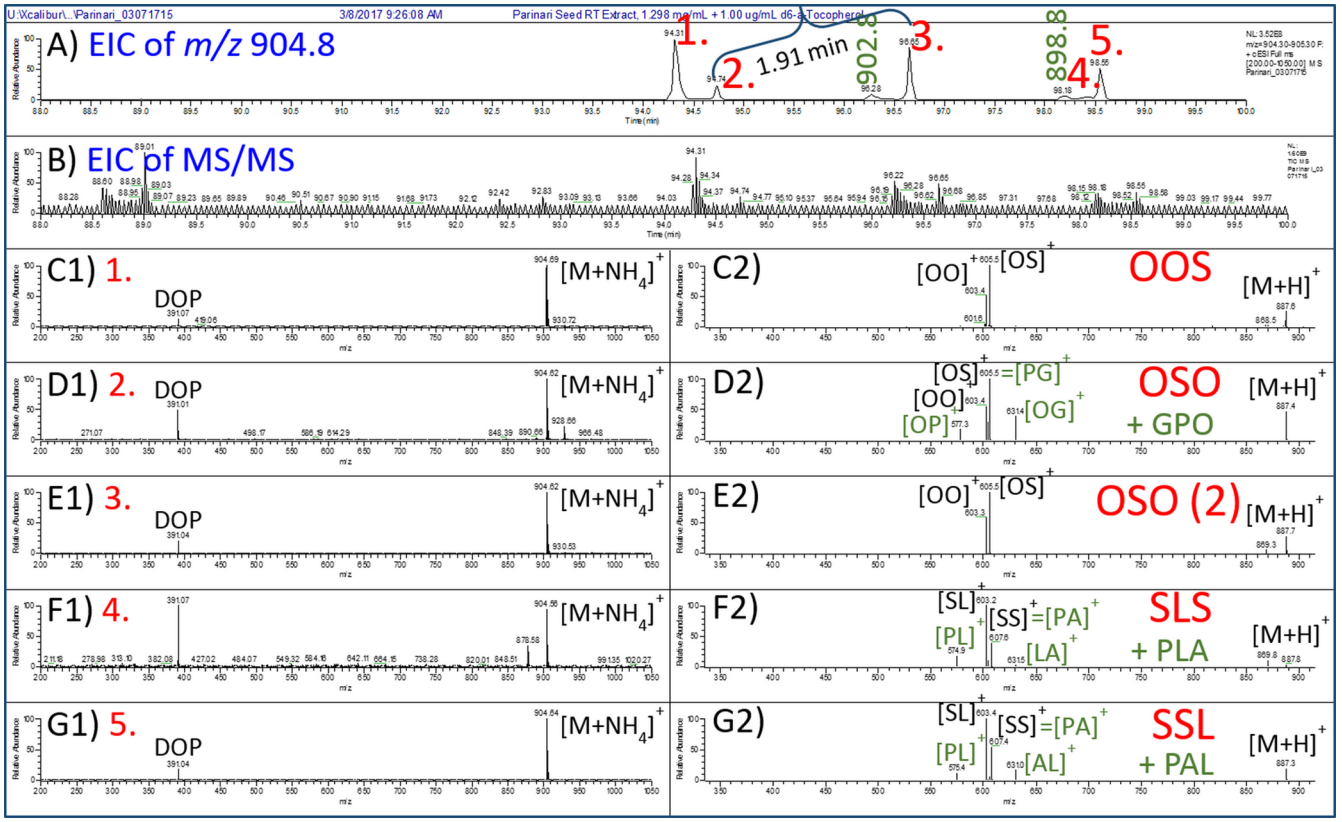

Figure 9. Extracted ion chromatograms and mass spectra of *m*/*z* 904.8 by Ag-ion UHPLC ESI-MS and MS/MS showing differentiation of regioisomers. DOP: dioctyl phthalate (plasticizer). FA abbreviations are in the Experimental Section.

An interesting observation that was unique to PSO was the difference in the ratios of the intact DAG peaks shown in Table 3 (in the column labeled DAG pk. 2/1). In most seed oils, the 1,2 + 2,3-DAG peak elutes earlier and is ∼2 times larger than the 1,3-DAG peak, which is smaller and elutes just after the larger peak. In PSO, even normal DAGs like LL showed a larger second peak as well as El-containing DAGs like ElEl and EllL and oxo-DAGs, oxo-ElEl, oxo-EllL, etc.

Another interesting observation was that APCI-MS and MS/MS spectra of di-El containing TAGs (ElElEl, ElElL, ElElO, etc.) showed almost exclusively the $[ElEl]^+$ $[DAG]^+$, *m*/*z* 595.5, with very little of the $[ElX]^+$ $[DAG]^+$ fragment. This unique behavior may indicate the possibility of cross-linking of the di-El FA chains during ionization in the APCI source, making it energetically unfavorable for formation of the $[ElX]^+$ fragment. This possibility was also indicated by the appearance of more of a *m*/*z* 593 fragment in ESI-MS/MS and APCI-MS mass spectra (Figures 4 and 5) than is formed from normal LnLnLn, which forms virtually only the expected *m*/*z* 595.5. Furthermore, TAGs containing oxElEl behaved in a similar manner, producing *m*/*z* 609.5 with little or no $[EllL]^+$, $[ElO]^+$, or other related $[DAG]^+$ fragments, as in Figure 4.

Finally, some readers may believe that this system of two chromatographs with four mass spectrometers is prohibitively complex or expensive and cannot readily be replicated. We want to point out that researchers may take aspects of the experiments that are needed and leave unnecessary parts behind. If we had only one mass spectrometer for the ^{1}D, we would use the HRAM Q Exactive Orbitrap instrument in APCI-MS mode. This would still allow identification of unknowns by HRAM MS, while also allowing quantification of FSVs, most of which do not respond well to ESI-MS without derivatization. Some may not be interested in 2D-LC at all, but the demonstration of Ag-ion UHPLC can be applied to standalone UHPLC in new ways. This arrangement of experiments was not expensive, because the slow ^{2}D chromatography and maintaining and repairing instruments ourselves allows us to keep older, inexpensive instruments in service, providing valuable data long after they have been retired elsewhere. The WCCCS system was not at all expensive, makes switching between instruments in experiments very easy, and would be a valuable addition to any LC-MS lab. Thus, while we demonstrated an unprecedented series of experiments that employ a novel arrangement of instruments, many of the components and concepts can be taken and applied individually to address a wide variety of analytical problems.

CONCLUSIONS

This work represents the first report of an application employing comprehensive 2D-LC with quadruple parallel mass spectrometry, or LC1MS2 × LC1MS2, for an LC2MS4 approach. Also reported here are the first examples of production of a silver-ion UHPLC column for triacylglycerol analysis, Ag-ion UHPLC, and Ag-ion UHPLC used as the ^{2}D in comprehensive 2D-LC. This work provides the first description of intact DAGs and TAGs from *P. curatellifolia* seed oil, of an oxo-FA in *P. curatellifolia* along with its confirmation using HRAM ESI-MS and GC-MS, and the first quantification of oxo-DAGs and oxo-TAGs for PSO. APCI-MS data provided indications of unique ionization and fragmentation mechanisms occurring in the APCI source for TAGs containing conjugated *trans* double bonds. This work provides the first quantification

DOI: 10.1021/acs.analchem.7b02753
Anal. Chem. 2017, 89, 10537−10546

of tocopherols in *P. curatellifolia* and shows the benefit of an extract-and-shoot approach for tocopherols in cherry pit oil. Further, these experiments describe the use of slow comprehensive 2D-LC, in which the problem of undersampling is bypassed by direct detection using six detectors in the ^{1}D. This allowed more flexibility in ^{2}D method development and instruments to be used that were older than those in conventional fast 2D-LC. The Ag-ion UHPLC column was ideal for separation of TAGs by type of double bond (*cis* versus *trans*) and of regioisomers based on the locations of unsaturated FAs, either in the 1,3 positions or the *sn*-2 position. These experiments employed a unique wireless communication contact closure system to coordinate all instruments.

■ ASSOCIATED CONTENT

Supporting Information

The Supporting Information is available free of charge on the ACS Publications website at DOI: 10.1021/acs.analchem.7b02753.

Experimental details for the Folch extraction, FAME preparation, GC-FID, and GC-MS analysis conditions, HPLC and UHPLC systems, and all mass spectrometers; external standard results for tocopherols by APCI-MS and internal standard and external standard results by UV detection; detailed compositions of FAMEs, DAGs, and TAGs for PSO, CPO, and SBO; and ^{2}D UHPLC contour plots for CPO and SBO (PDF)

■ AUTHOR INFORMATION

Corresponding Author

*E-mail: C.Byrdwell@ars.usda.gov.

ORCID

William C. Byrdwell: 0000-0001-8241-428X

Notes

The author declares no competing financial interest.

■ ACKNOWLEDGMENTS

The work of Dr. Robert Goldschmidt to extract the oil and perform the analysis of fatty acid methyl esters by GC-FID and confirmation of identities by GC-MS is gratefully acknowledged. The work of Mr. Lucas Stolp and Dr. Dharma Kodali to provide the CPO sample is gratefully acknowledged. This work was supported by the USDA Agricultural Research Service. Mention or use of specific products or brands does not represent or imply endorsement by the USDA.

■ REFERENCES

(1) Dugo, P.; Cacciola, F.; Kumm, T.; Dugo, G.; Mondello, L. *J. Chromatogr. A* **2008**, *1184*, 353−368.
(2) Malerod, H.; Lundanes, E.; Greibrokk, T. *Anal. Methods* **2010**, *2*, 110−122.
(3) Bedani, F.; Schoenmakers, P. J.; Janssen, H. G. *J. Sep. Sci.* **2012**, *35*, 1697−1711.
(4) Donato, P.; Cacciola, F.; Tranchida, P. Q.; Dugo, P.; Mondello, L. *Mass Spectrom. Rev.* **2012**, *31*, 523−559.
(5) Cacciola, F.; Donato, P.; Mondello, L.; Dugo, P. In *Handbook of Advanced Chromatography/Mass Spectrometry Techniques*; Holčapek, M., Byrdwell, W. C., Eds.; Elsevier/AOCS Press: Champaign, IL, 2017; pp 350−450.
(6) Stoll, D. R. In *Handbook of Advanced Chromatography/Mass Spectrometry Techniques*; Holčapek, M., Byrdwell, W. C., Eds.; Elsevier/AOCS Press: Champaign, IL, 2017; pp 250−350.
(7) Marriott, P. J.; Schoenmakers, P.; Wu, Z. Y. *LC-GC Eur.* **2012**, *25*, 1.
(8) Schoenmakers, P.; Marriott, P.; Beens, J. *LC-GC Eur.* **2003**, *16*, 335−339.
(9) Davis, J. M.; Stoll, D. R.; Carr, P. W. *Anal. Chem.* **2008**, *80*, 461−473.
(10) Mondello, L.; Tranchida, P. Q.; Stanek, V.; Jandera, P.; Dugo, G.; Dugo, P. *J. Chromatogr. A* **2005**, *1086*, 91−98.
(11) Dugo, P.; Kumm, T.; Crupi, M. L.; Cotroneo, A.; Mondello, L. *J. Chromatogr. A* **2006**, *1112*, 269−275.
(12) Dugo, P.; Kumm, T.; Chiofalo, B.; Cotroneo, A.; Mondello, L. *J. Sep. Sci.* **2006**, *29*, 1146−1154.
(13) van der Klift, E. J. C.; Vivó-Truyols, G.; Claassen, F. W.; van Holthoon, F. L.; van Beek, T. A. *J. Chromatogr. A* **2008**, *1178*, 43−55.
(14) Yang, Q.; Shi, X.; Gu, Q.; Zhao, S.; Shan, Y.; Xu, G. *J. Chromatogr. B: Anal. Technol. Biomed. Life Sci.* **2012**, *895*−*896*, 48−55.
(15) Wei, F.; Ji, S. X.; Hu, N.; Lv, X.; Dong, X. Y.; Feng, Y. Q.; Chen, H. *J. Chromatogr. A* **2013**, *1312*, 69−79.
(16) Hu, J.; Wei, F.; Dong, X. Y.; Lv, X.; Jiang, M. L.; Li, G. M.; Chen, H. *J. Sep. Sci.* **2013**, *36*, 288−300.
(17) Bang, D. Y.; Moon, M. H. *J. Chromatogr. A* **2013**, *1310*, 82−90.
(18) Holčapek, M.; Ovčačíková, M.; Lísa, M.; Cífková, E.; Hájek, T. *Anal. Bioanal. Chem.* **2015**, *407*, 5033−5043.
(19) Byrdwell, W. C. *Anal. Bioanal. Chem.* **2011**, *401*, 3317−3334.
(20) Christie, W. W. *J. High Resolut. Chromatogr.* **1987**, *10*, 148−150.
(21) Ogungbenle, H. N.; A, A. A. *Br. Biotechnol. J.* **2014**, *4*, 379−386.
(22) Abolaji, O. A.; Adebayo, A. H.; Odesanmi, O. S. *Pak. J. Nutr.* **2007**, *6*, 665−668.
(23) Chisholm, M. J.; Hopkins, C. Y. *J. Am. Oil Chem. Soc.* **1966**, *43*, 390−392.
(24) Cornelius, J. A.; Hammonds, T. W.; Leicester, J. B.; Ndabahweji, J. K.; Rosie, D. A.; Shone, G. G. *J. Sci. Food Agric.* **1970**, *21*, 49−50.
(25) Sommerfeld, M. *Prog. Lipid Res.* **1983**, *22*, 221−233.
(26) Byrdwell, W. C. *J. Lab. Autom.* **2014**, *19*, 461−467.
(27) Korlesky, N. M.; Stolp, L. J.; Kodali, D. R.; Goldschmidt, R.; Byrdwell, W. C. *J. Am. Oil Chem. Soc.* **2016**, *93*, 1−11.
(28) Byrdwell, W. C.; Neff, W. E.; List, G. R. *J. Agric. Food Chem.* **2001**, *49*, 446−457.
(29) Byrdwell, W. C.; Emken, E. A.; Neff, W. E.; Adlof, R. O. *Lipids* **1996**, *31*, 919−935.
(30) Byrdwell, W. C. *J. Chromatogr. A* **2013**, *1320*, 48−65.
(31) Ball, G. F. M. *Fat-Soluble Vitamin Assays in Food Analysis: A Comprehensive Review*; Elsevier Science Publishing: New York, 1988.
(32) Matos, J. T. V.; Duarte, R. M. B. O.; Duarte, A. C. *J. Chromatogr. B: Anal. Technol. Biomed. Life Sci.* **2012**, *910*, 31−45.
(33) Place, B. J.; Morris, M. J.; Phillips, M. M.; Sander, L. C.; Rimmer, C. A. *J. Chromatogr. A* **2014**, *1368*, 107−115.
(34) Cook, D. W.; Rutan, S. C.; Stoll, D. R.; Carr, P. W. *Anal. Chim. Acta* **2015**, *859*, 87−95.
(35) Donato, P.; Rigano, F.; Cacciola, F.; Schure, M.; Farnetti, S.; Russo, M.; Dugo, P.; Mondello, L. *J. Chromatogr. A* **2016**, *1458*, 54−62.
(36) Morris, L. J. *J. Lipid Res.* **1966**, *7*, 717−732.
(37) Byrdwell, W. C. *Anal. Bioanal. Chem.* **2015**, *407*, 5143−5160.
(38) Byrdwell, W. C. *J. Am. Oil Chem. Soc.* **2015**, *92*, 1533−1547.
(39) Fauconnot, L.; Hau, J.; Aeschlimann, J. M.; Fay, L. B.; Dionisi, F. *Rapid Commun. Mass Spectrom.* **2004**, *18*, 218−224.
(40) Powell, W. S. *Anal. Biochem.* **1981**, *115*, 267−277.
(41) Byrdwell, W. C.; Neff, W. E. *J. Liq. Chromatogr. Relat. Technol.* **1998**, *21*, 1485−1501.
(42) Byrdwell, W. C.; Neff, W. E. *Rapid Commun. Mass Spectrom.* **2002**, *16*, 300−319.

DOI: 10.1021/acs.analchem.7b02753
Anal. Chem. 2017, 89, 10537−10546

Supporting Information for

Comprehensive Dual Liquid Chromatography with Quadruple Mass Spectrometry (LC1MS2×LC1MS2 = LC2MS4) for Analysis of *Parinari Curatellifolia* and Other Seed Oil Triacylglycerols

William C. Byrdwell*

U.S.D.A., Agricultural Research Service, Beltsville Human Nutrition Research Center, Food Composition and Methods Development Lab, 10300 Baltimore Ave., Bldg. 161, Beltsville, MD 20705.

Contents of Supporting Information:

- More detailed RFN DAG composition of *Parinari curatellifolia* seed oil extract (Table S-19)
- RFN DAG composition of SBO by APCI-MS (Table S-20)

8. Detailed compositions of TAGs for CPO, PSO, and SBO.
   - Detailed RFN triacylglycerol (TAG) composition of CPO by APCI-MS (Table S-21)
   - Detailed RFN TAG composition of PSO by APCI-MS (Table S-22)
   - Detailed RFN TAG composition of SBO by APCI-MS (Table S-23)
9. ^{2}D UHPLC contour plot for CPO.
   - ^{2}D UHPLC Plots for CPO by APPI-MS on TSQ Quantum Access Max mass spectrometer (Fig. S-4)
   - ^{2}D UHPLC Plots for CPO by ESI-MS on LCQ Deca XP mass spectrometer (Fig. S-5)
10. ^{2}D UPHLC contour plot for SBO.
   - ^{2}D UHPLC Plots for SBO by APPI-MS on TSQ Quantum Access Max mass spectrometer (Fig. S-6)
   - ^{2}D UHPLC Plots for SBO by ESI-MS on LCQ Deca XP mass spectrometer (Fig. S-7)

---

1. Experimental Section

Chemicals

a) Boron Trifluoride (BF_3) – 14 % in methanol obtained from Sigma-Aldrich (St. Louis, MO).
b) Chloroform – Sigma-Aldrich 99.9 % A.C.S. HPLC grade.
c) Dichloromethane (DCM) – Fisher Scientific (Pittsburgh, PA) Optima grade.
d) Ethanol (EtOH) – Sigma-Aldrich 100 % (200 proof) HPLC/Spectrophotometric grade.
e) Isooctane (2,2,4-trimethyl pentane) – Mallinckrodt (Paris, KY).
f) Methanol (MeOH) – Fisher Scientific Optima LC/MS grade.
g) Potassium chloride (KCl) – certified A.C.S. grade obtained from Fisher Scientific.
h) Sodium chloride (NaCl) – A.C.S. reagent grade obtained from Sigma (St. Louis, MO).
i) Sodium Hydroxide (NaOH) – A.C.S. reagent grade obtained from Aldrich (Milwaukee, WI).
j) Water – Obtained from in-house Millipore (Bedford, MA) Milli-Q Water Purification System.

Qualitative Standards

a) Multi-component FAME Standard - GLC Reference Standard 68B from Nu-Check Prep (Elysian, MN) contains 18 FAME derivatives of fatty acids ranging from C14 to C24 and was prepared as a solution at 100 mg in 50 mL isooctane.
b) Multi-component FAME Standard – GLC Reference Standard 14B from Nu-Check Prep contains the FAME derivatives of the five odd carbon number unsaturated fatty acids from C13:0 to C21:0. It was prepared as a solution at 100 mg in 50 mL isooctane.
c) Methyl Tricosanoate (FAME derivative of C23:0 fatty acid) – Obtained from Nu-Check Prep and prepared as a solution at 15 mg in 25 mL isooctane.
d) Methyl Pentacosanoate (FAME derivative of C25:0 fatty acid) – Obtained from Santa Cruz Biotechnology, Inc. (Dallas, TX) and prepared as a solution at 15 mg in 25 mL isooctane.
e) Methyl hexacosanoate (FAME derivative of C26:0 fatty acid) – Obtained from Matreya LLC (Pleasant Gap, PA) and prepared as a solution at 15 mg in 25 mL isooctane.

Folch Extraction of *Parinari curatellifolia* Seeds

Parinari curatellifolia seeds were obtained from Top Tropicals (Ft. Myers, FL). Seeds were placed in a -80 °C freezer for two hours. The hard, thick shells were then cracked with a hammer, and the inner, white endosperms were obtained. The average seed mass, including the shell, was 5.2 g, and the average recovered portion was 0.41 g, or about 8 % of the total. The endosperms were ground in an electric grinder. The resulting oily meal was collected, and 0.2 g portions were weighed for extraction. The extraction of Folch *et al.*[1] was performed using two successive 4 mL portions of 2:1 chloroform: methanol. For the initial portion stirring was for 20 min. Samples were then centrifuged at 1000 rpm for 2 min and the supernatant was recovered. This procedure was then repeated, but for the second portion stirring was for 5 min. The recovered extracts were

combined and washed with 2 mL of aqueous 0.1 % KCl. A final centrifugation at 1000 rpm for 2 min was performed, and the lower, chloroform layers were collected. Solvent evaporation to constant mass was performed at room temperature under a stream of nitrogen gas. The final, oily residues obtained were on average 45 % by mass of the ground portions weighed for extraction. A solution of 67.6 mg PSO in 50 mL de-aerated (da-) dichloromethane (DCM) / methanol (MeOH) (1:1), = 1.352 mg/mL, was initially prepared and kept at -2 °C. Later, this solution was brought to room temperature and 25.0 mL was transferred to a 25.0 mL flask, 1.0 mL was removed, and 1.0 mL of 25.0 μg/mL d_6-α-tocopherol internal standard (IS) was added to give 1.298 mg/mL *P. curatellifolia* with 1.0 μg/mL IS.

The CPO was obtained by hexane Soxhlet extraction as previously described.[2] 1.3768 mg was added to an amber volumetric flask, ~30 mL of da-DCM/MeOH (1:1) was added with swirling, 4.0 mL of 25.0 μg/mL d_6-α-tocopherol IS was added, and the solution was made to 100 mL with da-DCM/MeOH (1:1) to give 1.3768 mg/mL oil with 1.0 μg/mL IS.

An 8 fluid ounce bottle of organic wild soybean (Glycine soja) oil (SBO) with an expiration date of 11/2019 was purchased from an online marketplace and was used as received. A solution of 1.3162 mg/mL SBO with 1.0 μg/mL d_6-α-tocopherol IS was prepared the same way as the CPO.

2. FAME Preparation of Oil Samples and GC Analysis

For all oil samples FAME derivatives were prepared as described in **AOCS Official Method Ce 1b-89** with the following modifications:

a) The parts of the method related to the absolute determination of eicosapentaenoic acid (EPA) and docosahexaenoic acid (DHA) were omitted.
b) The entire procedure was performed at room temperature (22 °C). Saponification with 0.5 M methanolic NaOH was overnight (16 – 20 hrs), and BF_3 treatment was for 45 - 60 min.
c) For each sample, two extractions using 1 mL isooctane for each were performed; however, the evaporation of the combined extracts to 1 mL was omitted.

GC Apparatus

a) GC column – Supelco (Bellefonte, PA) Omegawax 250, 30 m x 0.25 mm x 0.25 μm film thickness.
b) Gas Chromatograph – Agilent Technologies (Santa Clara, CA) 6890N GC with G2613A injector, split/splitless inlet, flame ionization detector (FID), and using OpenLab CDS ChemStation Edition for GC Systems (Rev. C.01.05 [35]) software.
c) GC-MS – Agilent Technologies 5975C Inert XL EI/CI MSD with 7890A GC System and G4513A injector, split/splitless inlet, and using MassHunter GC/MS Acquisition (B.07.00 SP1.1549) software.

GC-FID Method

The GC-FID method was as described in **AOCS Official Method Ce 1b-89** with the following specifications and modifications:

a) Carrier gas – Helium with operation in constant flow mode at 1 mL/min.
b) FID – Temperature set at 270 °C with hydrogen flow at 45 mL/min, air flow at 450 mL/min, and make-up gas (Nitrogen) flow at 45 mL/min.
c) Inlet – Temperature set at 250 °C; 1 μL injection; operation in split mode at 50:1 split.
d) Oven – Initial temperature of 170 °C, temperature gradient of 1 °C/min to 250 °C.
e) Run Time – 80 min.

GC-MSD Method

The GC part of the GC-MSD method was similar to that described above for the GC-FID method. Total ion current chromatograms were acquired in scanning mode from *m/z* 50 to m/z 450 at 1.9 scans/second and a step size of 0.1 *m/z*. Samples were run using electron ionization (EI) mode and again using positive ion chemical ionization (CI) mode with methane reagent gas.

3. HPLC and MS Instruments and Conditions

A) Agilent 1200 HPLC *(Agilent Technologies, Santa Clara, CA)*

Solvent module with membrane degasser (G1379B), quaternary pump (G1311A), autosampler (G1329A) with 1290 thermostat (G1330B) at 15 °C, thermostatted column compartment (G1316A), diode array detector (DAD) SL (G1315C), two-channel 24-bit analog-to-digital converter #1 (ADC) (35900E).

Two Inertsil ODS-2 columns in series, 25 cm × 4.6 mm, 5 µm particles (GL Sciences, Torrance, CA, USA) joined by a circularly bent 7-cm piece of 0.007 in. i.d. stainless steel tubing.

Columns were maintained at 10 °C throughout. 20 µL of standards and samples injected.

I. ^{1}D Gradient elution as follows:

1) Fat-soluble vitamin (FSV) standards:

Table S-1. ^{1}D HPLC gradient for fat-soluble vitamins.

Time (min)	%A (MeOH)	%B (ACN)	%C (EtOH)	%D (DCM)
0.0	95.0	0.0	5.0	0.0
25.0	95.0	0.0	5.0	0.0
30.0	60.0	0.0	15.0	25.0
40.0	65.0	0.0	10.0	25.0
50.0	65.0	0.0	10.0	25.0
51.0	95.0	0.0	5.0	0.0
54.0	95.0	0.0	5.0	0.0

2) Seed oil extracts:

Table S-2. ^{1}D HPLC gradient for seed oil extracts.

Time (min)	%A (MeOH)	%B (ACN)	%C (EtOH)	%D (DCM)
0.0	95.0	0.0	5.0	0.0
25.0	95.0	0.0	5.0	0.0
30.0	60.0	0.0	15.0	25.0
40.0	65.0	0.0	10.0	25.0
50.0	65.0	0.0	10.0	25.0
70.0	65.0	0.0	10.0	25.0
90.0	50.0	0.0	25.0	25.0
100.0	35.0	0.0	40.0	25.0
110.0	30.0	0.0	45.0	25.0
118.0	30.0	0.0	45.0	25.0
120.0	95.0	0.0	5.0	0.0
130.0	95.0	0.0	5.0	0.0

II. ^{1}D Detector settings:

Table S-3. ^{1}D HPLC detector settings.

^{1}D Diode Array Detector (DAD)				
Wavelength (λ_{nm})	**Bandwidth ($\Delta\lambda_{nm}$)**	**Reference λ_{nm}**	**Reference $\Delta\lambda_{nm}$**	**Analyte(s)**
210	5	360	100	Generic
248	9	360	100	Phylloquinone (Vit. K_1)
265	9	360	100	Vitamin D_2 & D_3
297	11	450	100	Tocopherols (Vit. E)
326	11	450	100	Retinol (Vit. A), Retinyl Acetate, Retinyl Palmitate

^{1}D Fluorescence Detector (FLD)		
Excitation Wavelength (λ_{nm})	**Emission Wavelength (λ_{nm})**	**Analyte(s)**
Zero order [Xe lamp: 200-1200 nm]	310	α-Tocopheryl Acetate
Zero order (all λ)	330	Tocopherols (Vit. E)
Zero order (all λ)	420	Fluorescent 18:4-containing TAG reported in *Parinari glaberrimum*
Zero order (all λ)	470	Retinol (Vit. A), Retinyl Acetate, Retinyl Palmitate

^{1}D Corona Charged Aerosol Detector (CAD)	
Parameter	**Setting**
Range	20 pA
Filter	3
Power function	1.00
Gas (Nitrogen)	35 psi
Output offset	0%

^{1}D Evaporative Light Scattering Detector (ELSD) – Not Reported due to temporary signal failure	
Parameter	**Setting**
Evaporator	80 ^{o}C
Nebulizer	90 ^{o}C
Gas (Nitrogen)	1.20
Photomultiplier	8.4
Data Rate	40 Hz
Smoothing	5

B) Agilent 1290 UHPLC *(Agilent Technologies, Santa Clara, CA)*

Solvent module with membrane degasser, Infinity binary pump (G4220A), Infinity autosampler (G4226A - disconnected) with FC/ALS Thermostat (G1330B), thermostatted column compartment (G1316C), Infinity diode array detector (DAD) (G4212A), 8-port, 2-position, 1200 bar column-switching valve (G1170A).
Lab-made Ag-Ion column from ES Industries strong cation exchange column (Epic-SCX, #122191-ESCX), 10.0 cm × 2.1 mm, 3 µm, 120 Å, particles (ES Industries, West Berlin, NJ, USA).
Column was maintained at 10 °C throughout. Gradient stop time 1.86 min. Modulation time 1.91 min.

I. ^{2}D Shifted gradient elution as follows:

1) Fat-soluble vitamin (FSV) standards:

Table S-4. ^{2}D UHPLC shifted gradient for fat-soluble vitamins. See Figure S-1.

	^{2}D Time (min)				
^{1}D Time (min)	**0.00**	**0.55**	**1.5**	**1.70**	**1.80**
0.0	100.0	100.0	90.0	90.0	100.0
40.0	100.0	100.0	90.0	90.0	100.0
50.0	100.0	100.0	10.0	10.0	100.0
60.0	100.0	100.0	35.0	35.0	100.0
70.0	100.0	100.0	60.0	60.0	100.0
120.0	100.0	100.0	90.0	90.0	100.0
130.0	100.0	100.0	90.0	90.0	100.0

Time programmed exactly as 130 min run for seed oils to ensure identical gradient, and OpenLab ChemStation automatically truncated runs at 54 min.

2) Cherry (*Prunus cerasus*) and *Parinari curatellifolia* seed oil extracts:

Table S-5. ^{2}D UHPLC shifted gradient for cherry and parinari seed oil extracts. See Figure S-2.

	^{2}D Time (min)				
^{1}D Time (min)	**0.00**	**0.55**	**1.5**	**1.70**	**1.80**
0.0	100.0	100.0	90.0	90.0	100.0
40.0	100.0	100.0	90.0	90.0	100.0
50.0	100.0	100.0	10.0	10.0	100.0
60.0	100.0	100.0	35.0	35.0	100.0
70.0	100.0	100.0	60.0	60.0	100.0
120.0	100.0	100.0	90.0	90.0	100.0
130.0	100.0	100.0	90.0	90.0	100.0

3) Commercial wild soybean (*Glycine soja*) oil:

Table S-6. ^{2}D UHPLC shifted gradient for cherry and parinari seed oil extracts. See Figure S-3.

	^{2}D Time (min)				
^{1}D Time (min)	**0.00**	**0.55**	**1.5**	**1.70**	**1.80**
0.0	100.0	100.0	95.0	95.0	100.0
40.0	100.0	100.0	95.0	95.0	100.0
50.0	100.0	100.0	25.0	10.0	100.0
60.0	100.0	100.0	40.0	35.0	100.0
70.0	100.0	100.0	90.0	90.0	100.0
120.0	100.0	100.0	95.0	95.0	100.0
130.0	100.0	100.0	95.0	95.0	100.0

II. ^{2}D Detector settings:

Table S-7. ^{2}D HPLC detector settings (Identical to ^{1}D DAD settings).

^{2}D Diode Array Detector (DAD)				
Wavelength (λ_{nm})	Bandwidth ($\Delta\lambda_{nm}$)	Reference λ_{nm}	Reference $\Delta\lambda_{nm}$	Analyte
210	5	360	100	Generic
248	9	360	100	Phylloquinone (Vit. K_1)
265	9	360	100	Vitamin D_2 & D_3
297	11	450	100	Tocopherols (Vit. E)
326	11	450	100	Retinol (Vit. A), Retinyl Acetate, Retinyl Palmitate

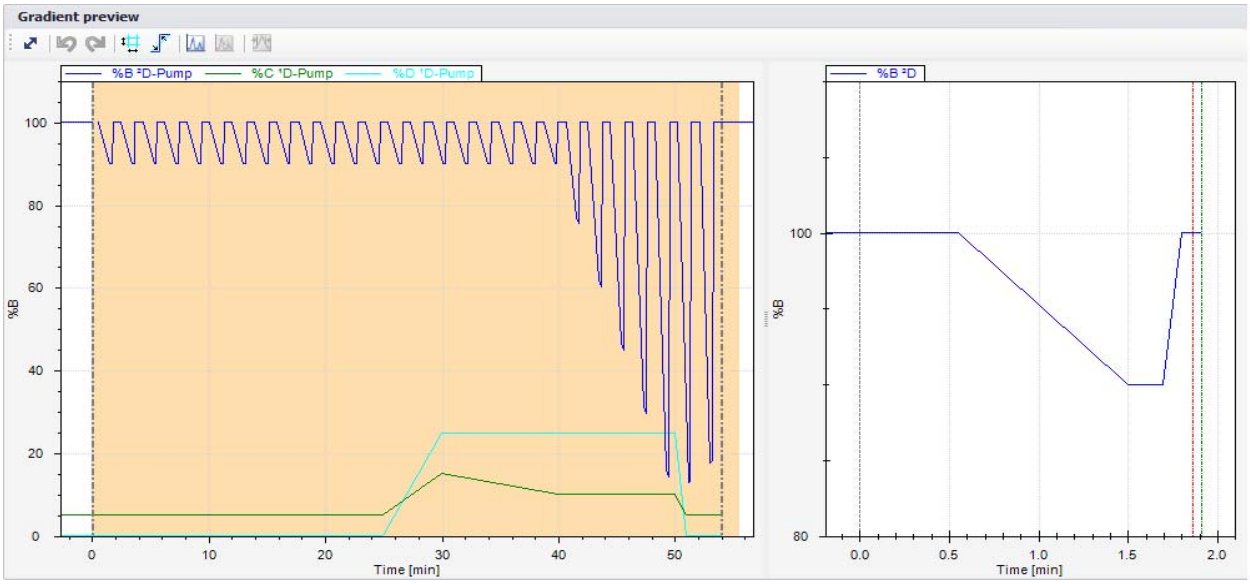

Figure S-1. ^{2}D UHPLC shifted gradient for fat-soluble vitamins. See Table S-4.

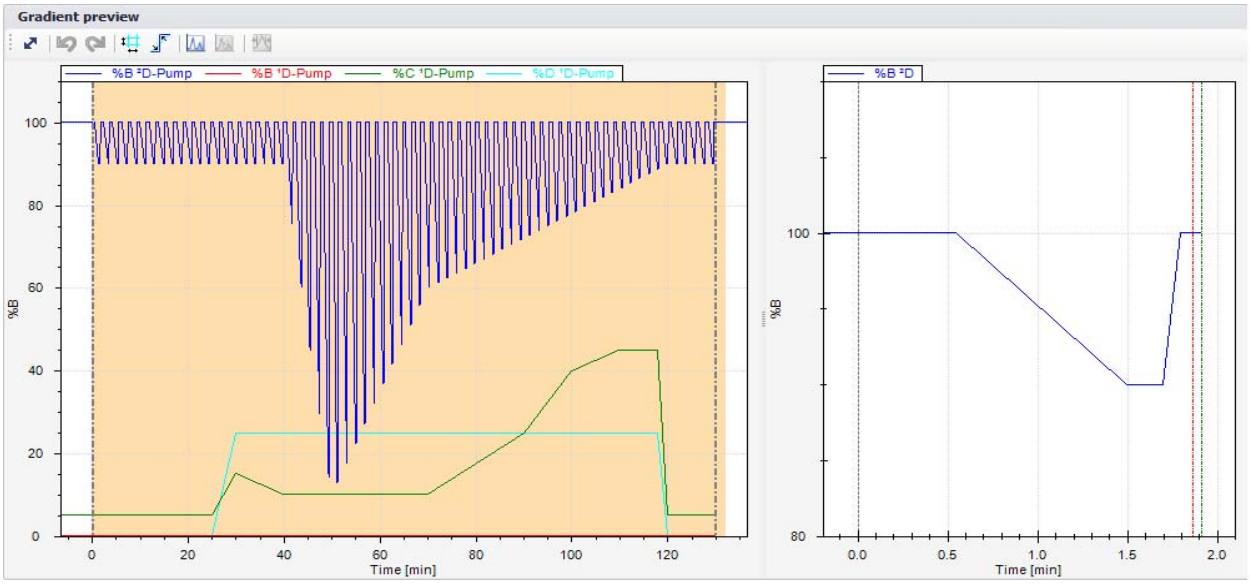

Figure S-2. ^{2}D UHPLC shifted gradient for cherry and parinari seed oil extracts. See Table S-5.

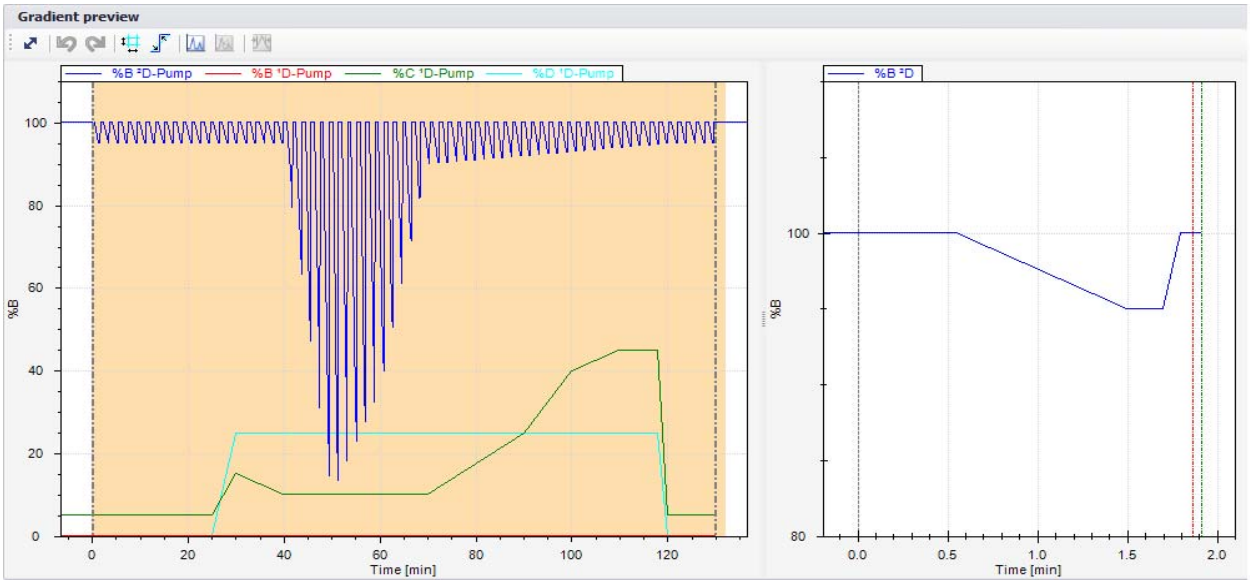

Figure S-3. ^{2}D UHPLC shifted gradient for commercial wild soybean (*Glycine soja*) samples. See Table S-6.

4. Mass Spectrometer Operating Conditions

A) ^{1}D HPLC detection.

Table S-8. QExactive high resolution accurate mass Orbitrap™ mass spectrometer (Thermo Fisher Scientific, San Jose, CA, USA) for qualitative ^{1}D HPLC analysis.

All runs use ammonium formate (NH_4OCOH) in methanol (1:4) at 20 μL/min supplied by Applied Biosystems AB140C dual piston syringe pump.

Fat-Soluble Vitamin Analysis			
Full-Scan ESI-MS		**Data-Dependent Acquisition (DDA) MS/MS**	
Parameter	**Setting**	**Parameter**	**Setting**
Source parameters	See below	In-source CID	0.0 eV
Run time	54 min	Precursor resolution	140,000
In-source CID	45.0 eV	Product resolution	70,000
Resolution	140,000	Precursor scan range	*m/z* 300-750
Scan range	*m/z* 200-2000	Loop	Top 2 precursors
AGC target	3e6	Isolation window	1.0 *m/z*
Max. inj. time	200 ms	Norm. collision energy	50
Mode	Centroid	Max. inj. time	Pre:100 ms/Prod:50 ms
Polarity	+ and -		

Cherry and Parinari Extract 130 min Analysis			
Up to 44 min same as FSV above. Soybean Oil the same, but first segment = 50 min.			
Full-Scan ESI-MS		**TAG DDA MS/MS**	
Parameter	**Setting**	**Parameter**	**Setting**
Sheath gas (Nitrogen)	25	In-source CID	0.0 eV
Auxiliary gas (Nitrogen)	0	Resolution	Pre:140,000/Prod:70,000
Sweep gas	0	Precursor scan range	*m/z* 700-1100
Spray voltage	4000 V	Loop	Top 2 precursors
Capillary temp.	250 °C	Isolation window	1.0 *m/z*
Run time	130 min	Norm. collision energy	15
In-source CID	45.0 eV	**DAG DDA MS/MS**	
Resolution	140,000	In-source CID	**80.0 eV**
Scan range	*m/z* 200-2000	Resolution	Pre:140,000/Prod:70,000
AGC target	3e6	Precursor scan range	*m/z* 350-750
Max. inj. time	200 ms	Loop	Top 3 precursors
Mode	Centroid	Isolation window	1.0 *m/z*
Polarity	+ and -	Norm. collision energy	35

Table S-9. TSQ Vantage EMR tandem sector quadrupole mass spectrometer (Thermo Fisher Scientific, San Jose, CA, USA). Multi-segment qualitative and SIM and SRM quantitative analysis parameters for ^{1}D HPLC.

Fat-Soluble Vitamin Analysis

APCI Source Parameters

Parameter	Setting
Vaporizer heater	400 °C
Sheath gas (Nitrogen)	50
Auxiliary gas (Nitrogen)	5
Sweep gas	0
Capillary temp.	250 °C
Declustering voltage	0 V

1.0 mTorr Argon collision induced dissociation (CID) gas turned on throughout all scans.
All scans except precursor scans used Q3. All used 0.7 FWHM peak widths unless otherwise stated.
All scans were in (+) ion mode with centroided masses.

Segment 1 (0-2 min)	
Scan event 1. Q3 Full-scan MS	
Scan range	*m/z* 200-2000
Scan time	1.8 s
Scan events 2. & 3. DDA MS/MS	
Signal threshold	1e4
Scan time	1.0 s
Collision energy	19 V
Repeat	Top 2 precursors

Segment 2 (2-18 min)		
Scan event 1. Full-scan MS same as Segment 1		
Scan event 2. 1 DDA MS/MS same as Segment 1		
Scan event 3. Q3 Selected Ion Monitoring (**SIM**)		
0.5 s scan time	0.5 scan width	
m/z	**Analyte**	
269.227	All retinols	
287.238	Retinol (Vit. A)	
301.217	Retinoic Acid	
329.248	Retinyl Acetate	
Scan event 4. Selected Rxn. Monitoring (**SRM**)		
Scan time 0.5 s	Scan width 0.5	CID 19 V
Precursor (*m/z*)	**Product (*m/z*)**	**Analyte**
269.227	93.070	Retinol
301.217	159.123	Retinoic Acid
329.248	269.227	Ret. Acetate

Segment 3 (18-36 min)		
Scan event 1. Full-scan MS same as Segment 1		
Scan event 2. DDA MS/MS same as Segment 1		
Scan event 3. Q3 Selected Ion Monitoring (**SIM**)		
0.5 s scan time	0.5 scan width	
m/z	**Analyte**	
385.347	Cholecalciferol (Vit. D_3)	
397.347	Ergocalciferol (Vit. D_2)	

Segment 3 - Scan Event 3 – SIM Continued	
m/z	**Analyte**
403.358	δ-Tocopherol
416.365	γ,β-Tocopherol $[M]^{+}\cdot$
417.373	γ,β-Tocopherol $[M+H]^{+}$
431.389	α-Tocopherol
437.427	d_6-α-Tocopherol

Scan event 4. Selected Reaction Monitoring (**SRM**)		
Scan time 0.5 s	Scan width 0.5	CID 19 V
Precursor (*m/z*)	**Product (*m/z*)**	**Analyte**
385.347	367.337	Vitamin D_3
397.347	379.337	Vitamin D_2
403.358	137.122	δ-Tocopherol
416.365	151.133	γ,β-Tocopherol
417.373	151.133	γ,β-Tocopherol
431.389	165.149	α-Tocopherol
437.427	171.167	d_6-α-Tocopherol

Segment 4 (36-44 min)	
Scan event 1. Full-scan MS same as Segment 1	
Scan event 2. 1 DDA MS/MS same as Segment 1	
Scan event 3. Q3 Selected Ion Monitoring (**SIM**)	
0.5 s scan time	0.5 scan width
m/z	**Analyte**
451.358	Phylloquinone (Vit. K_1)
473.400	α-Tocopheryl Acetate

Scan event 4. Selected Reaction Monitoring (**SRM**)		
Scan time 0.5 s	Scan width 0.5	CID 19 V
Precursor (*m/z*)	**Product (*m/z*)**	**Analyte**
451.358	187.240	Vitamin K_1
473.400	207.250	α-Toco. Acetate

Segment 5 (44-54 min)
Identical to Segment 4 for these analyses.
SIM and SRM for β-Carotene removed.

Table S-10. TSQ Vantage EMR tandem sector quadrupole mass spectrometer (Thermo Fisher Scientific, San Jose, CA, USA). Multi-segment qualitative and SIM and SRM quantitative analysis parameters for ^{1}D HPLC analysis.

Cherry and Parinari Seed Oil Extract Analysis			
APCI Source Parameters – Same as for FSV given in Table 9			
1.0 mTorr Argon CID gas turned on throughout all scans. All scans except precursor scans used Q3 with 0.7 FWHM peak widths unless otherwise stated. All scans were in (+) ion centroid mode.			
Segment 1 (0-2 min)		**Segment 5 (44-130 min)**	
Scan event 1. Same Full-Scan MS as for FSV.		**Scan event 1.** Same Full-Scan MS as for FSV.	
Scan event 2. Same 1 DDA MS/MS as for FSV.		**Scan event 2.** Narrow range full-scan MS of TAGs	
Scan event 3. Same DDA MS/MS as for FSV.		Scan range	*m/z* 800-1100
Segment 2 (2-18 min)		Scan time	0.40 s
Scan event 1. Same Full-Scan MS as for FSV.		**Scan event 3.** DDA MS/MS of TAGs	
Scan event 2. Same 1 DDA MS/MS as for FSV.		Signal threshold	1e4
Scan event 3. Same 4 x **SIM** as for FSV.		Scan time	1.0 s
Scan event 4. Same 3 x **SRM** as for FSV.		Collision energy	30 V
Segment 3 (18-36 min)		Repeat	Top precursor only
Scan event 1. Same Full-Scan MS as for FSV.		**Scan event 4.** Narrow range MS of $[DAG]^{+}$	
Scan event 2. Same 1 DDA MS/MS as for FSV.		Scan range	*m/z* 400-750
Scan event 3. Same 7 x **SIM** as for FSV.		Scan time	0.45 s
Scan event 4. Same 7 x **SRM** as for FSV.		**Scan event 5.** DDA MS/MS of $[DAG]^{+}$	
Segment 4 (36-44 min)		Signal threshold	1e4
Scan event 1. Same Full-Scan MS as for FSV.		Scan time	0.75 s
Scan event 2. Same 1 DDA MS/MS as for FSV.		Collision energy	40 V
Scan event 3. Same 2 x **SIM** as for FSV.		Repeat	Top precursor only
Scan event 4. Same 2 x **SRM** as for FSV.		**Segment 5. 54-130 min for Soybean Oil only.**	

B) ^{2}D UHPLC detection.

Table S-11. TSQ Quantum Access Max tandem sector quadrupole mass spectrometer (Thermo Fisher Scientific, San Jose, CA, USA). Full-scan MS for ^{2}D UHPLC qualitative analysis.

Fat-Soluble Vitamin and Seed Oil Extract Analysis	
APPI Source Parameters	
Parameter	**Setting**
Vaporizer heater	400 °C
Sheath gas (Nitrogen)	60
Auxiliary gas (Nitrogen)	5
Sweep gas	0
Capillary temp.	270 °C
Skimmer offset	10 V

1.0 mTorr Argon CID gas turned on throughout all scans. All scans except precursor scans used Q3. All used 0.7 FWHM peak widths unless otherwise stated. All scans were in (+) ion centroid mode.
All runs use acetone dopant at 20 μL/min by Applied Biosystems AB140B dual piston syringe pump.

Scan event 1. Q3 Full-scan MS		**Scan events 2. Data-dependent MS/MS**	
Scan range	*m/z* 150-2000	Signal threshold	1e4
Scan time	1.0 s	Scan time	0.9 s
Runt time 53.50 min for FSVs. Run time 129.50 min for seed oil extracts.		Collision energy	50 V
		Repeat	Top precursor only

Table S-12. LCQ Deca XP hyperbolic ion trap mass spectrometer (Thermo Fisher Scientific, San Jose, CA, USA). Full-scan MS for ^{2}D UHPLC qualitative analysis.

Fat-Soluble Vitamin and Seed Oil Extract Analysis			
APPI Source Parameters			
Parameter		**Setting**	
Sheath gas (Nitrogen)		35	
Auxiliary gas (Nitrogen)		5	
Capillary temp.		265 °C	
Spray Voltage		5000 V	
All scans were in (+) ion mode with centroided masses. All runs use ammonium formate (NH_4OCOH) in methanol (1:4) at 20 μL/min supplied by Applied Biosystems AB140C dual piston syringe pump.			
Scan event 1. Full-scan MS		**Scan events 2&3. Data-dependent MS/MS**	
Scan range	*m/z* 200-1050	Signal threshold	1e4
Scan time	1.0 s	Precursor range	*m/z* 200-1050
Runt time 54.0 min for FSVs. Run time 130.0 min for seed oil extracts.		Norm. Coll. Energy	45.0%
		Activation Q	0.350
		Activation time	900 ms
		Isolation width	2.0 *m/z*
		Repeat	Top 2 precursor

5. External standard results for tocopherols by APCI-MS, internal standard and external standard results by UV detection.

Table S-13. Internal and external standard results by UV detection and external standard results by SIM and SRM APCI-MS from ^{1}D HPLC, in ppm (= μg/g oil).

	Internal Standard Method									
		α-Toco	SD	r^2	γ-Toco	SD	r^2	δ-Toco	SD	r^2
Cherry	UV	217	22	0.9765	636	14	0.9662	151	10	0.9893
Parinari	UV	5427[a]	104		616	31				
Soybean	UV				193	19		205	12	
	External Standard Method									
		α-Toco	SD	r^2	γ-Toco	SD	r^2	δ-Toco	SD	r^2
Cherry	UV	217	22	0.9765	717	17	0.9738	118	13	0.9947
	SIM	278	18	0.9898	583	13	0.9766	98.0	5.1	0.9762
	SRM	244	21	0.9328	717	40	0.9459	126	10	0.9324
Parinari	UV	5427[a]	104		688	39				
	SIM	643.3	1.6		705	27				
	SRM	631	95		849	127				
Soybean	UV				168	24		186	15	
	SIM	30.8	1.8		150.8	4.3		213	11	
	SRM	42.0	1.2		174.2	6.9		187	17	

[a]This value highlights the danger of interfering species in UV detection.

Table S-14. Limits of detection (LOD) and limits of quantification (LOQ) calculated from calibration lines. Observed LOD and LOQ (*e.g.* from sequential dilution) are likely lower.

	Internal Standard Method			
		α-Toco (ppm)	**γ-Toco (ppm)**	**δ-Toco (ppm)**
LOD[a]	**UV**	200	15	44
b+3*$\sigma_{0.125}$	**SIM**	7.5	79	99
	SRM	6.5	42	23
LOQ[b]	**UV**	668	51	146
b+10*$\sigma_{0.125}$	**SIM**	25	264	330
	SRM	22	139	76
	External Standard Method			
		α-Toco (ppm)	**γ-Toco (ppm)**	**δ-Toco (ppm)**
LOD[a]	**UV**	200	36	71
b+3*$\sigma_{0.125}$	**SIM**	25	59	81
	SRM	20	39	13
LOQ[b]	**UV**	668	120	235
b+10*$\sigma_{0.125}$	**SIM**	82	196	271
	SRM	68	131	42

[a]Limit of Detection (LOD) area (E.S.) or ratio (I.S.) = (intercept (b) + 3 x standard deviation of lowest standard [0.125 μg/mL]) put into calibration equation and converted to ppm (=μg/g oil).

[b]Limit of Quantification (LOQ) area (E.S.) or ratio (I.S.) = (intercept (b) + 10 x standard deviation of lowest standard [0.125 μg/mL]) put into calibration equation and converted to ppm (=μg/g oil).

The results for UV detection of α-tocopherol in Table S-14 demonstrate the shortcomings of UV detection in real samples. Any other sterols or other molecules that absorb at all at the wavelength of 297 nm in the time range around 33.8 min will contribute to the peak area attributed to α-tocopherol. For instance, the second peak of di-eleosteroyl diacylglycerol, ElEl = *m/z* 595.5 $[DAG]^+$ and *m/z* 613.5 $[M+H]^+$, eluted overlapped with α-tocopherol (both at 33.78 min by APCI-MS) and was present in a much larger amount than α-tocopherol. Therefore, even a small absorbance of 18:3 at 297 nm would skew the results for α-tocopherol, as observed. By both SIM and SRM APCI-MS this overlap presented no problem.

It is important to note that both internal standard and external standard UV and APCI-MS approaches showed higher levels of tocopherols than were observed in the results from the commercial labs previously presented. Thus, all of these approaches, when coupled to an extract-and-shoot sample preparation approach, identified larger amounts of tocopherols than were found using the commonly used heated saponification, extraction and collection, followed by derivatization approach widely used.[3] Even when cherry kernels were analyzed without saponification and derivatization, the amount of tocopherols varied greatly with extraction conditions,[4] with the extraction of Folch *et al.*[1] commonly considered the 'gold standard'.[5]

Of course, as we previously reported with vitamin D, UV data should not be trusted without MS data to prove that the peaks are pure. And if not pure, as in the case of α-tocopherol, UV data should not be used for quantification.

On the other hand, as with vitamin D,[6] if MS data can be used to prove that the peaks are pure, UV data may be more sensitive and show lower standard deviations than APCI-MS, since APCI inherently has more chemical noise associated with the ionization process. This is demonstrated by the lower LOD and LOQ for γ-tocopherol in Table S-14, since these values are based on the standard deviation in the lowest standard (0.125 μg/mL).

6. Detailed compositions of FAMEs for PSO, CPO, and SBO.

Table S-15. Detailed response factor normalized and GC-FID fatty acid compositions of *Parinari curatellifolia* seed oil, including compositions of isomers of 18:3 (CN:db) and oxo-eleostearic acid.

	Parinari Seed Oil (PSO)					
	APPI-MS	**SD**	**GC-FID**			
M (14:0)	0.000%	0.000%	0.033%			
Po (16:1)	0.020%	0.001%	0.018%			
P (16:0)	9.136%	0.042%	9.287%		**GC-FID**	**SD**
El (all 18:3)	48.768%	0.096%	48.840%	α-El	90.00%	0.07%
L (18:2)	14.379%	0.137%	13.992%	β-El	7.63%	0.06%
O (18:1)	17.709%	0.060%	17.518%	Ln	0.09%	0.00%
S (18:0)	7.267%	0.113%	7.589%	18:3x1	1.70%	0.04%
A (20:0)	0.402%	0.006%	0.395%	18:3x2	0.38%	0.01%
G (20:1)	0.688%	0.014%	0.695%	18:3x3	0.14%	0.01%
21:0	0.003%	0.000%	0.000%	18:3x4	0.06%	0.01%
B (22:0)	0.031%	0.000%	0.032%		100.00%	
23:0	0.005%	0.000%	0.014%		**GC-FID**	**SD**
Lg (24:0)	0.022%	0.001%	0.033%	oxo-El-1	3.60%	0.49%
25:0	0.004%	0.000%	0.012%	oxo-El-2	81.01%	0.76%
Ce (26:0)	0.003%	0.000%	0.000%	oxo-El-3	2.07%	0.34%
oxo-El	1.563%	0.017%	1.543%	oxo-El-4	13.32%	0.30%
Sum	100.000%		100.000%		100.00%	

Table S-16. Detailed response factor normalized and GC-FID fatty acid compositions of cherry pit oil (not including isomers).

Cherry Pit Oil (CPO)			
FA	**APCI-MS**	**SD**	**GC-FID**
M	0.006%	0.000%	0.069%
Po	0.629%	0.030%	0.626%
P	8.841%	0.120%	8.324%
El	5.766%	0.115%	5.760%
L	32.650%	0.243%	33.320%
O	47.825%	0.203%	47.598%
S	2.437%	0.011%	2.507%
A	0.943%	0.008%	0.916%
G	0.423%	0.002%	0.405%
21	0.015%	0.001%	0.015%
B	0.208%	0.001%	0.202%
23	0.025%	0.001%	0.031%
Lg	0.193%	0.006%	0.187%
25	0.017%	0.001%	0.022%
Ce	0.022%	0.001%	0.018%
Sum	100.000%		100.000%

Table S-17. Detailed response factor normalized and GC-FID fatty acid compositions of soybean oil (not including isomers, discussed below).

Soybean Oil (SBO)			
FA	**APCI-MS**	**SD**	**GC-FID**
M	0.002%	0.000%	0.094%
Po	0.098%	0.009%	0.102%
P	12.109%	0.064%	11.953%
Ln	7.406%	0.103%	7.519%
L	52.699%	0.474%	51.515%
O	22.369%	0.189%	23.619%
S	4.286%	0.113%	4.175%
A	0.336%	0.008%	0.323%
G	0.197%	0.005%	0.184%
21	0.023%	0.000%	0.021%
B	0.341%	0.012%	0.329%
23	0.016%	0.000%	0.032%
Lg	0.106%	0.005%	0.102%
25	0.005%	0.000%	0.008%
Ce	0.007%	0.001%	0.021%
Sum	100.000%		100.000%

GC-FID FA compositions were determined from the weight percentage of fatty acid methyl esters (FAME) and converted from weight percent FAME to mole percent FA.

As expected, the composition in Table S-16 is in excellent agreement to the FA composition given for CPO previously.[2] Similarly, the FA composition for wild SBO (*Glycine soja*) is in excellent agreement with the composition of SBO from a dietary supplement recently reported using the 'dilute-and-shoot' approach with quadruple parallel mass spectrometry.[7]

7. Detailed compositions of diacylglycerols for CPO, PSO, and SBO.

Table S-18. Diacylglyerol (DAG) composition of CPO by response factor normalized APCI-MS.

Cherry Pit Oil (CPO)			
DAG	**% Comp.**	**SD**	**2/1**
ElEl	0.03%	0.01%	0.62
LEl	1.11%	0.07%	0.66
LL	18.14%	0.56%	0.47
OEl	0.54%	0.02%	0.54
PoO	0.19%	0.04%	0.64
PoP	0.57%	0.10%	0.54
OL	28.72%	1.62%	0.35
PL	12.06%	1.06%	0.23
OO	22.40%	1.14%	0.28
OP	11.38%	0.13%	0.28
SL	2.98%	0.09%	0.29
OS	1.89%	1.64%	0.26
Sum	100.00%		
DAG/TAG	1.08%	±0.03%	

Table S-19. More detailed diacylglycerol (DAG) composition of *Parinari curatellifolia* seed oil extract by response factor normalized APCI-MS.

Parinari Seed Oil (PSO)			
DAG	**% Comp.**	**SD**	**2/1**
oxEloxEl	0.02%	0.00%	
oxEoEo	0.75%	0.07%	0.21
oxEoL	0.10%	0.01%	0.28
oxEoO	0.17%	0.01%	**0.23**
oxEoP	0.10%	0.01%	0.30
ElEl	17.91%	0.62%	2.57
LEl	11.25%	0.10%	2.72
LL	11.49%	0.10%	4.19
OEl	12.60%	0.30%	1.57
PoO	0.75%	0.03%	1.61
PoP	0.06%	0.01%	1.37
OL	14.53%	0.45%	3.43
PL	6.73%	0.10%	1.53
OO	6.87%	0.17%	1.50
OP	6.91%	0.11%	0.72
SL	4.72%	0.17%	1.59
OS	5.03%	0.14%	0.52
Sum	100.00%		
DAG/TAG	1.52%	±0.05%	

Table S-20. Diacylglycerol (DAG) composition of SBO by response factor normalized APCI-MS.

Soybean Oil (SBO)			
DAG	**% Comp.**	**SD**	**2/1**
LnLn	0.49%	0.07%	0.34
LLn	7.29%	0.19%	0.54
LL	43.73%	1.39%	0.56
OLn	1.02%	0.18%	0.40
PoO	0.00%	0.00%	
PoP	0.03%	0.01%	0.71
OL	15.84%	1.20%	0.39
PL	15.78%	0.37%	0.20
OO	4.90%	0.22%	0.26
OP	3.93%	0.07%	0.29
SL	5.33%	0.10%	0.27
OS	1.67%	0.08%	0.26
Sum	100.00%		
DAG/TAG	1.39%	±0.04%	

8. Detailed compositions of TAGs for CPO, PSO, and SBO.

Table S-21. Detailed triacylglycerol (TAG) composition of CPO by response factor normalized APCI-MS. Structures shown here are not regiospecific.

Cherry Pit Oil (CPO)							
TAG	**RT**	**% Comp.**	**SD**	**TAG**	**RT**	**% Comp.**	**SD**
ElElEl	55.10	0.017%	0.001%	**LOA**	94.47	0.880%	0.021%
ElElL	56.80	0.634%	0.012%	**LLB**	94.98	0.153%	0.002%
LLEl	58.46	5.377%	0.066%	**POS**	95.97	0.380%	0.003%
LLL	60.33	3.964%	0.025%	**PLA**	96.46	0.218%	0.009%
ElElO	62.14	0.211%	0.008%	**SSL**	96.54	0.112%	0.003%
ElElP	63.32	0.040%	0.003%	**OL-21**	98.76	0.019%	0.001%
OLEl	64.22	4.258%	0.275%	**LL-23**	99.18	0.024%	0.000%
PLEl	65.50	2.044%	0.084%	**PPS**	99.76	0.001%	0.000%
LLO	66.35	13.434%	0.372%	**LElLg**	100.66	0.010%	0.000%
PoPL	67.27	0.902%	0.110%	**SOG**	101.77	0.018%	0.005%
LLP	67.76	3.506%	0.044%	**OOA**	102.36	0.755%	0.015%
ElElG	68.73	0.002%	0.000%	**OLB**	102.64	0.178%	0.003%
MOL	69.53	0.019%	0.001%	**LLLg**	102.95	0.140%	0.003%
EoEoS	71.12	0.028%	0.002%	**POA**	104.27	0.202%	0.001%
OOEl	71.12	2.090%	0.017%	**SSO**	104.37	0.130%	0.002%
POEl	72.73	0.614%	0.009%	**PBL**	104.42	0.058%	0.001%
OOL	73.73	16.632%	0.332%	**SLA**	104.68	0.060%	0.002%
LLG	73.86	0.318%	0.016%	**OO-21**	105.87	0.012%	0.002%
POPo	74.81	0.992%	0.117%	**OL-23**	106.04	0.028%	0.001%
POL	75.42	7.442%	0.144%	**LL-25**	106.25	0.016%	0.001%
LLS	76.40	0.774%	0.018%	**OOB**	108.92	0.148%	0.005%
PPL	77.30	0.597%	0.012%	**OLLg**	109.10	0.167%	0.003%
LElA	79.60	0.027%	0.001%	**LLCe**	109.28	0.017%	0.000%
ElElA	80.13	0.002%	0.000%	**PLLg**	110.63	0.052%	0.004%
SOEl	82.46	0.989%	0.033%	**POB**	110.65	0.046%	0.002%
OOO	82.51	17.235%	0.247%	**SLB**	110.83	0.020%	0.001%
OLG	82.59	0.477%	0.004%	**SOA**	110.89	0.057%	0.004%
OOP	84.44	6.991%	0.153%	**OO-23**	111.81	0.023%	0.001%
PLG	84.54	0.193%	0.015%	**OL-25**	111.95	0.018%	0.000%
SLO	85.28	1.695%	0.011%	**OOLg**	114.76	0.152%	0.009%
LLA	86.08	0.622%	0.009%	**OLCe**	114.83	0.020%	0.002%
POP	86.51	0.606%	0.001%	**PLCe**	116.40	0.005%	0.000%
SLP	87.36	0.309%	0.003%	**POLg**	116.42	0.042%	0.002%
PPP	89.98	0.001%	0.000%	**SLLg**	116.79	0.009%	0.001%
LL-21	90.60	0.016%	0.001%	**SOB**	116.82	0.011%	0.002%
OOG	91.14	0.270%	0.002%	**OO-25**	117.64	0.016%	0.002%
ElOA	91.70	0.027%	0.003%	**OOCe**	120.56	0.018%	0.001%
LElB	92.27	0.012%	0.000%	**POCe**	122.44	0.006%	0.002%
OOS	93.82	2.332%	0.005%	**SOLg**	122.79	0.011%	0.001%
EoSS	93.98	0.066%	0.020%	**OOMo**	126.67	0.001%	0.000%
				Sum		99.999%	

Table S-22. Detailed triacylglycerol (TAG) composition of PSO by response factor normalized APCI-MS. TAG structures given are not regiospecific.

Parinari Seed Oil (PSO)							
TAG	**RT**	**% Comp.**	**SD**	**TAG**	**RT**	**% Comp.**	**SD**
oxEloxEloxEl	32.02	0.000%	0.000%	**ElEl-21**	84.80	0.008%	0.000%
oxEloxElEl	40.28	0.030%	0.001%	**SLO**	85.04	1.392%	0.062%
oxEloxElL	41.35	0.005%	0.000%	**LLA**	85.83	0.026%	0.001%
oxEloxElO	43.58	0.011%	0.000%	**POP**	86.29	0.528%	0.018%
oxEloxElP	43.91	0.011%	0.001%	**SLP**	87.09	0.930%	0.026%
oxElElEl	46.02	1.269%	0.019%	**ElElB**	89.30	0.032%	0.001%
oxElElL	47.08	0.384%	0.009%	**PPP**	89.64	0.022%	0.000%
oxEloxElS	47.38	0.013%	0.000%	**OOG**	90.98	0.071%	0.001%
oxElLL	48.20	0.034%	0.002%	**ElOA**	91.46	0.122%	0.010%
oxElElO	50.54	0.865%	0.006%	**LElB**	92.04	0.010%	0.000%
oxElElP	51.23	0.676%	0.022%	**ElEl-23**	93.65	0.011%	0.000%
oxElLO	51.87	0.085%	0.001%	**OOS**	93.68	0.845%	0.026%
oxElLP	52.56	0.043%	0.001%	**ElSS**	93.83	0.934%	0.023%
oxElOO	56.21	0.143%	0.004%	**LLB**	94.84	0.003%	0.000%
oxElElS	56.26	0.850%	0.018%	**POS**	95.79	0.747%	0.009%
oxElOP	56.83	0.058%	0.000%	**PLA**	96.36	0.136%	0.001%
oxElPP	57.75	0.008%	0.000%	**SSL**	96.38	0.400%	0.012%
oxElLS	57.85	0.047%	0.003%	**ElElLg**	97.90	0.028%	0.001%
oxElOS	63.36	0.060%	0.004%	**OL-21**	98.41	0.001%	0.000%
oxElSP	64.23	0.038%	0.001%	**LL-23**	98.96	0.001%	0.000%
oxElSS	72.40	0.019%	0.002%	**PPS**	99.31	0.051%	0.001%
ElElEl	55.11	12.036%	0.191%	**LElLg**	100.40	0.009%	0.000%
ElElL	56.70	8.252%	0.143%	**SOG**	101.83	0.043%	0.007%
LLEl	58.47	3.348%	0.092%	**ElEl-25**	101.83	0.008%	0.000%
LLL	60.31	0.405%	0.013%	**OOA**	102.10	0.030%	0.002%
ElElO	62.05	11.267%	0.153%	**OLB**	102.46	0.015%	0.001%
ElElP	63.23	8.090%	0.141%	**LLLg**	102.80	0.003%	0.000%
OLEl	64.10	7.790%	0.254%	**POA**	104.09	0.091%	0.002%
PLEl	65.44	4.556%	0.134%	**SSO**	104.19	0.339%	0.009%
LLO	66.33	1.018%	0.020%	**PBL**	104.37	0.012%	0.000%
PoPL	66.95	0.008%	0.001%	**SLA**	104.45	0.034%	0.001%
LLP	67.64	0.863%	0.024%	**ElElCe**	105.19	0.006%	0.000%
ElElG	68.65	1.274%	0.038%	**OL-23**	105.83	0.002%	0.000%
ElElS	70.83	8.941%	0.531%	**OOB**	108.76	0.004%	0.000%
OOEl	70.94	4.202%	0.118%	**OLLg**	108.88	0.008%	0.001%
POEl	72.50	3.003%	0.084%	**PLLg**	110.44	0.006%	0.000%
LLG	73.27	0.185%	0.042%	**SLB**	110.51	0.006%	0.001%
OOL	73.53	1.782%	0.048%	**SOA**	110.62	0.028%	0.001%
PPEl	74.35	0.429%	0.014%	**POB**	110.66	0.008%	0.000%
POPo	74.40	0.041%	0.002%	**OO-23**	111.52	0.002%	0.000%
POL	75.30	2.094%	0.033%	**OL-25**	111.75	0.002%	0.000%
LLS	76.15	0.484%	0.012%	**OOLg**	114.56	0.005%	0.000%
PPL	77.15	0.701%	0.012%	**OLCe**	114.71	0.002%	0.000%
LElA	79.48	0.277%	0.001%	**POLg**	116.16	0.003%	0.001%
ElElA	79.89	0.474%	0.010%	**PLCe**	116.35	0.001%	0.000%
SOEl	82.19	2.995%	0.100%	**SOB**	116.54	0.003%	0.000%
OOO	82.21	0.961%	0.018%	**SLLg**	116.57	0.003%	0.000%
OLG	82.29	0.342%	0.051%	**OO-25**	117.51	0.001%	0.000%
OOP	84.24	1.413%	0.030%	**POCe**	122.29	0.002%	0.001%
ElSP	84.32	0.974%	0.059%	**SOLg**	122.81	0.004%	0.002%
PLG	84.37	0.168%	0.045%	**Sum**		100.000%	

Table S-23. Detailed triacylglycerol (TAG) composition of SBO by response factor normalized APCI-MS. TAG structures are not regiospecific.

Soybean Oil							
TAG	**RT**	**% Comp.**	**SD**	**TAG**	**RT**	**% Comp.**	**SD**
LnLnLn	49.69	0.068%	0.002%	**LLB**	95.03	0.319%	0.004%
LnLnL	52.73	0.919%	0.012%	**POS**	95.97	0.560%	0.009%
LLLn	56.28	6.383%	0.026%	**PLA**	96.53	0.239%	0.007%
LnLnO	57.15	0.537%	0.118%	**SSL**	96.63	0.463%	0.017%
LnLnP	58.18	0.207%	0.007%	**LLnLg**	96.94	0.028%	0.001%
LLL	60.32	16.528%	0.303%	**OL-21**	98.69	0.022%	0.000%
OLLn	61.32	4.870%	0.130%	**LL-23**	99.14	0.027%	0.001%
PLLn	62.55	3.175%	0.097%	**PPS**	99.59	0.009%	0.000%
LLO	66.38	14.021%	0.518%	**OOA**	102.25	0.071%	0.004%
PoPL	66.99	0.009%	0.002%	**OLB**	102.68	0.183%	0.010%
OOLn	67.70	2.337%	0.017%	**LLLg**	102.91	0.093%	0.005%
LLP	67.75	12.466%	0.073%	**SSO**	104.28	0.165%	0.011%
PoOL	68.88	0.247%	0.022%	**POA**	104.32	0.092%	0.006%
POLn	68.95	1.274%	0.098%	**PBL**	104.38	0.181%	0.008%
PPLn	70.72	0.140%	0.008%	**SLA**	104.55	0.104%	0.005%
OOL	73.79	5.986%	0.094%	**OO-21**	105.81	0.008%	0.001%
LLG	73.89	0.262%	0.010%	**OL-23**	106.05	0.015%	0.000%
POPo	74.86	0.039%	0.006%	**LL-25**	106.37	0.008%	0.000%
POL	75.45	7.306%	0.040%	**OOB**	108.90	0.096%	0.005%
LLS	76.37	4.198%	0.048%	**OLLg**	109.08	0.057%	0.002%
PPL	77.28	2.301%	0.041%	**LLCe**	109.18	0.007%	0.001%
SOLn	77.91	0.409%	0.015%	**POB**	110.57	0.055%	0.003%
LLnA	78.93	0.057%	0.005%	**PLLg**	110.69	0.072%	0.003%
OOO	82.51	2.809%	0.131%	**SOA**	110.81	0.031%	0.002%
OLG	82.59	0.151%	0.004%	**SLB**	110.90	0.080%	0.004%
PLG	84.47	0.131%	0.020%	**OO-23**	111.80	0.006%	0.001%
OOP	84.47	2.620%	0.100%	**OL-25**	111.99	0.005%	0.000%
SLO	85.33	3.370%	0.198%	**OOLg**	114.74	0.031%	0.001%
LLA	86.07	0.247%	0.013%	**OLCe**	114.79	0.005%	0.001%
POP	86.45	0.641%	0.041%	**POLg**	116.40	0.015%	0.003%
SLP	87.37	1.736%	0.054%	**PLCe**	116.41	0.004%	0.000%
LLnB	88.32	0.091%	0.005%	**SLLg**	116.78	0.018%	0.001%
MOS	89.92	0.006%	0.001%	**SOB**	116.86	0.026%	0.002%
PPP	89.92	0.008%	0.000%	**OO-25**	117.68	0.002%	0.000%
LL-21	90.61	0.038%	0.001%	**OOCe**	120.50	0.002%	0.000%
OOG	91.23	0.054%	0.003%	**POCe**	122.58	0.001%	0.000%
OOS	93.80	1.068%	0.041%	**SLCe**	122.66	0.001%	0.000%
LOA	94.54	0.177%	0.007%	**SOLg**	122.86	0.007%	0.000%
				Sum		100.000%	

9. ^{2}D UHPLC Plots for cherry pit oil.

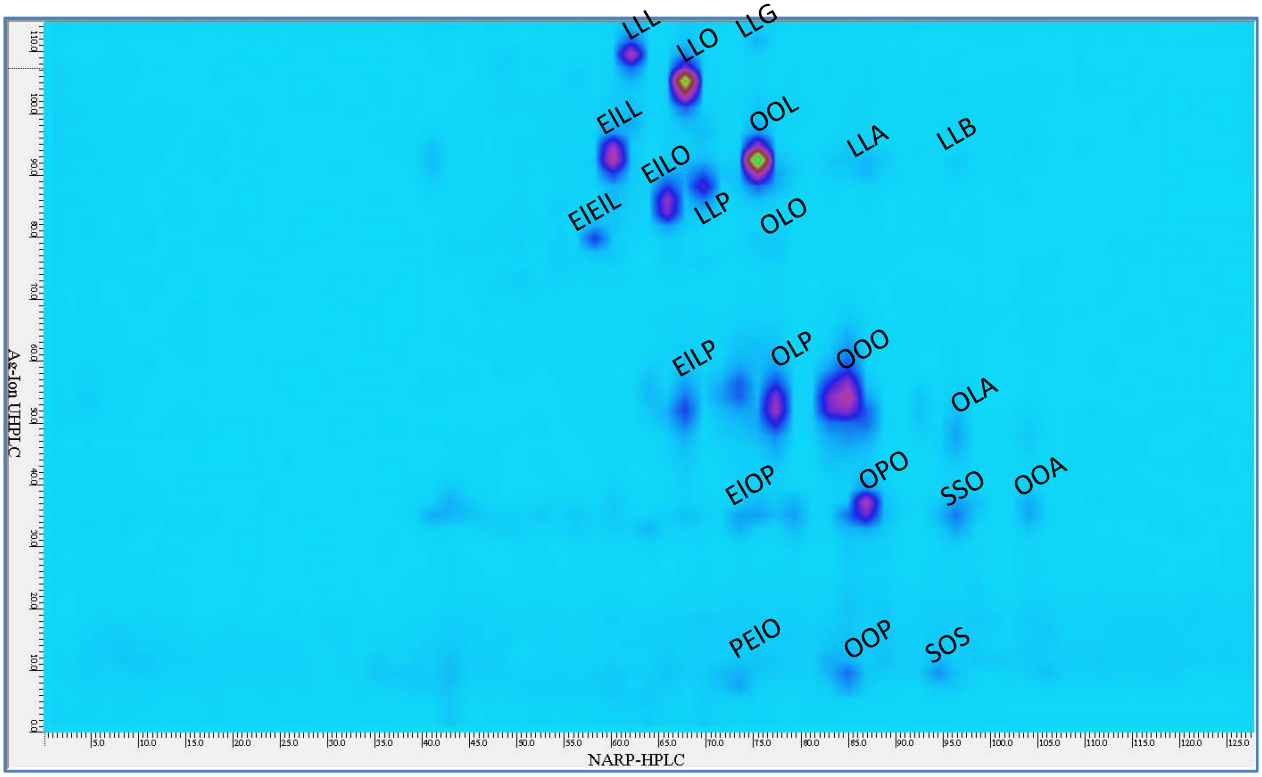

Figure S-4. ^{2}D UHPLC contour plot of cherry pit oil by APPI-MS on TSQ Quantum Access Max.

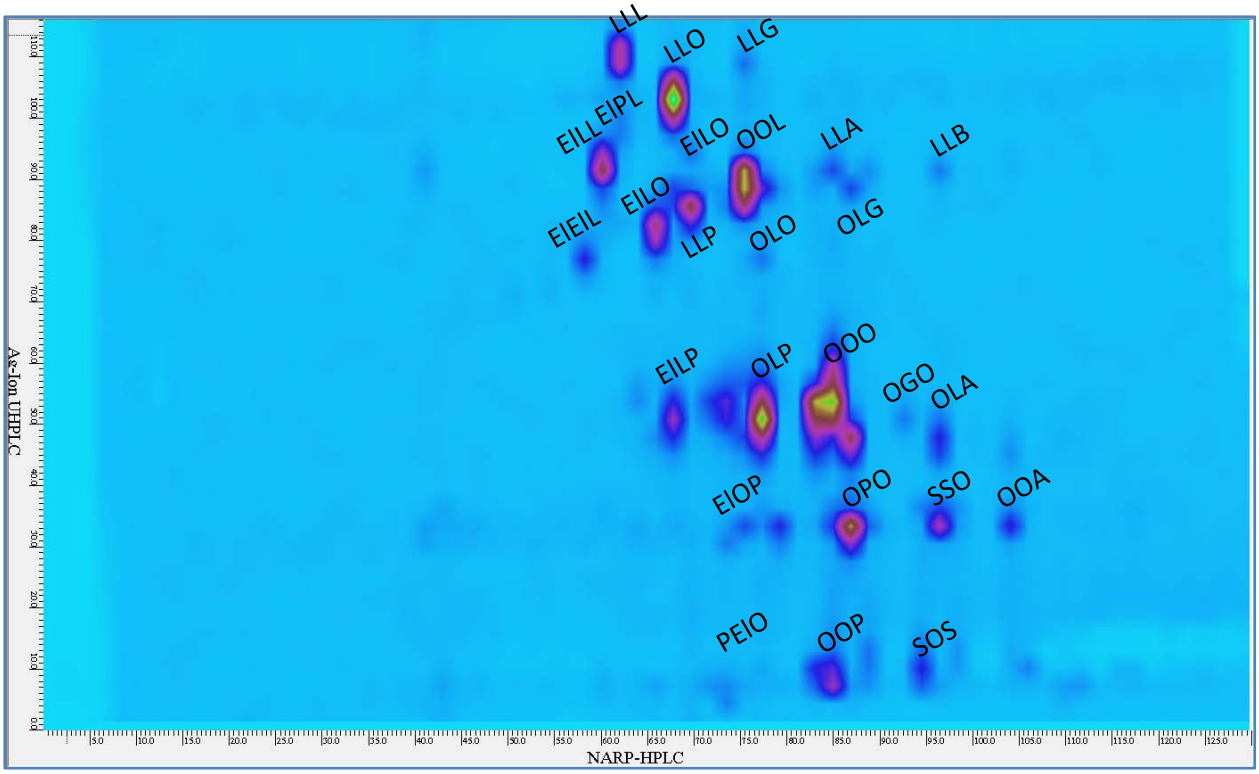

Figure S-5. ^{2}D UHPLC contour plot of cherry pit oil by ESI-MS on LCQ Deca XP.

10. ^{2}D UHPLC Plots for soybean oil.

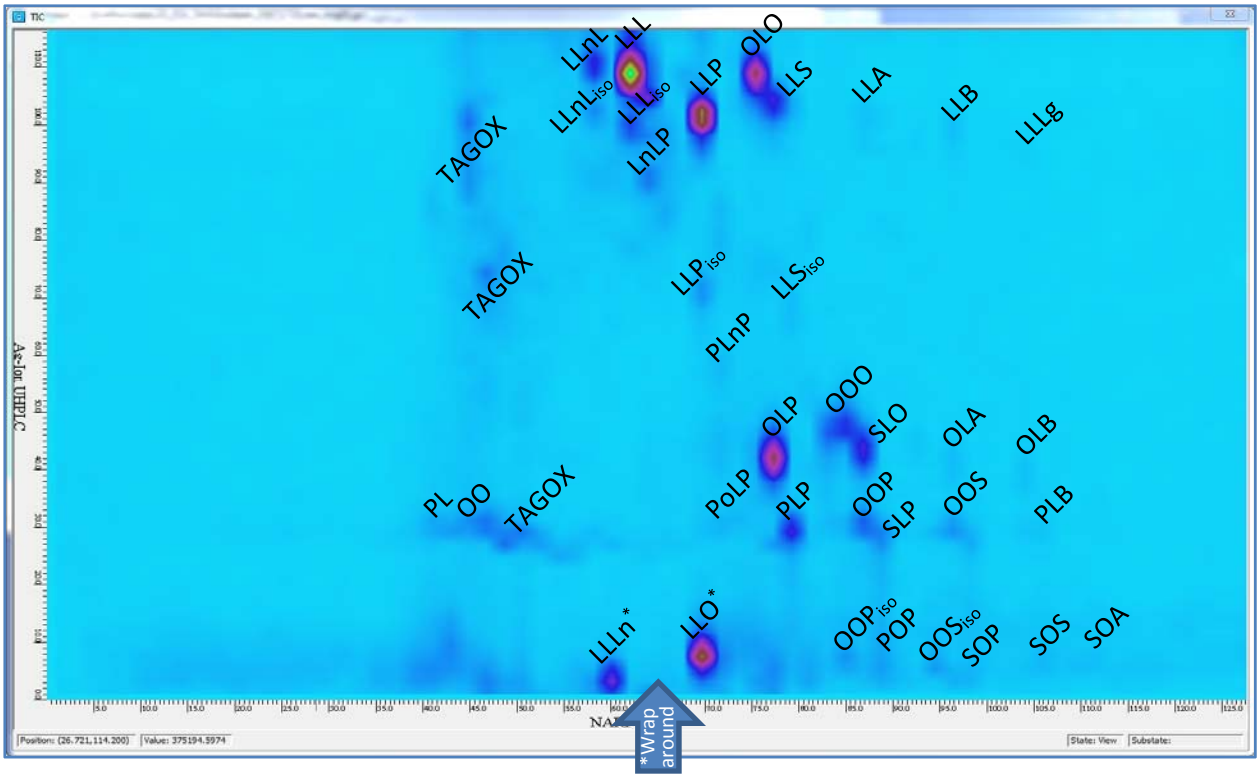

Figure S-6. ^{2}D UHPLC contour plot of soybean oil by APPI-MS on TSQ Quantum Access Max.

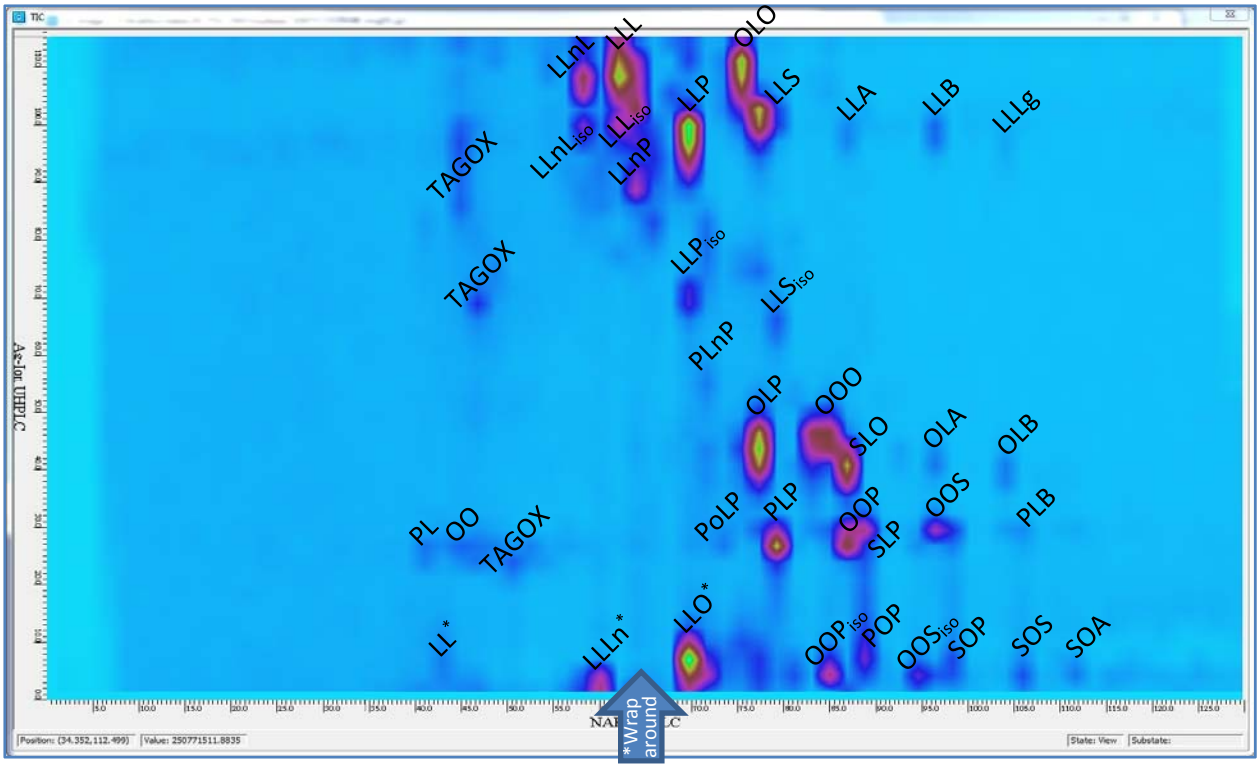

Figure S-7. ^{2}D UHPLC contour plot of soybean oil by ESI-MS on LCQ Deca XP.

Figures S-6 and S-7 show that TAGs with few degrees of unsaturation could be forced to be retained on the column longer by using a sharper reverse gradient, shown in Figure S-3. Notice the elution time of OLO in Figures S-6 and S-7 compared to OOL in Figures S-4 and S-5. However, LLLn and LLO experienced "wraparound" by eluting in the next modulation period, due to the lower ACN composition. Therefore, we have increased the ACN percentage to be intermediate between the gradient used for eleostearic acid-containing oils and this gradient. But we show these data to demonstrate the control that fine-tuning the ACN composition allows and because the quantification of the FSV and TAGs from the ^{1}D was unaffected.

The TAG identities are given by the masses of the $[M+NH_4]^+$ ions in ESI-MS spectra, and by $[M+H]^+$ and $[DAG]^+$ fragments in APPI-MS spectra. As we reported previously, the $[DAG]^+$ fragment ratios in ESI-MS and APPI-MS mass spectra are not as consistent for regioisomer identification as APCI-MS mass spectra.[8] Therefore, regioisomers identities for SBO were taken from our earlier report of SBO isomers[7] and were inferred from elution characteristics in the ^{2}D UHPLC chromatograms, not solely from $[DAG]^+$ ratios. APPI-MS has the distinct advantage that it is a non-contact ionization mode, unlike APCI-MS that accumulates a 'glob' of residue on the corona needle after extended exposure to solvents containing acetonitrile. But the $[DAG]^+$ fragment ratios are not as directly correlated with the regioisomeric positions of FAs in TAGs as in APCI-MS spectra. Thus, there is a trade-off in the use of APPI-MS versus APCI-MS.

The soybean oil analyzed for these experiments was a Halal SBO ordered from an online supplier, and showed higher levels of 18:3 isomers by GC-FID and GC-MS than most SBOs we have analyzed in the past, as well as some early-eluting TAG oxidation products (TAGOX). Normal linolenic acid represented 63.9% of all 18:3 species by GC-FID, another isomer was 15.8%, a third was 15.0%, and a fourth was 5.4%. Linoleic acid also showed isomers, with normal linoleic acid being 96.0% by GC-FID, one isomer being 2.1% and another being 1.9%. Two isomers of 18:1 were present, with oleic acid being 94.2% and the second isomer being 5.8%. Thus, Figures S-6 and S-7 show some of the minor TAG peaks labelled with "iso" to indicate additional isomer peaks. The combination of oxidation products and isomers may indicate that the oil was not stored properly prior to sale, or may indicate sample production or processing issues. Based on the current status of literature precedent, the ESI-MS and APPI-MS mass spectra were not sufficiently definitive to allow localization of the double bond positions. Of course, with adequate standards, the 2D-LC retention times could be used to identify the isomers, since, in many cases, they were separated on the new Ag-Ion UHPLC column. Since individual double bond isomers have not been specifically identified, the results for SBO FAs, DAGs, and TAGs in Tables S-17, S-20, and S-23, respectively, represent the sum of all isomers for each FA.

Supporting Information References

(1) Folch, J.; Lees, M.; Sloane-Stanley, G. H. *J. Biol. Chem.* **1957**, *226*, 497-509.
(2) Korlesky, N. M.; Stolp, L. J.; Kodali, D. R.; Goldschmidt, R.; Byrdwell, W. C. *J. Am. Oil Chem. Soc.* **2016**, 1-11.
(3) Slover, H. T.; Thompson, R. H.; Merola, G. V. *J. Am. Oil Chem. Soc.* **1983**, *60*, 1524-1528.
(4) Matthäus, B.; Özcan, M. M. *J. Food Lipids* **2009**, *16*, 187-199.
(5) Sheng, J.; Vannela, R.; Rittmann, B. E. *Bioresour. Technol.* **2011**, *102*, 1697-1703.
(6) Byrdwell, W. C. *J. Agric. Food Chem.* **2009**, *57*, 2135-2146.
(7) Byrdwell, W. C. *Anal. Bioanal. Chem.* **2015**, *407*, 5143-5160.
(8) Byrdwell, W. C. *J. Am. Oil Chem. Soc.* **2015**, *92*, 1533-1547.